Novel, Potent, and Selective 5-HT$_3$ Receptor Antagonists Based on the Arylpiperazine Skeleton: Synthesis, Structure, Biological Activity, and Comparative Molecular Field Analysis Studies

Maurizio Anzini,[‡] Andrea Cappelli,*[,‡] Salvatore Vomero,[‡] Gianluca Giorgi,[†] Thierry Langer,[∥] Michel Hamon,[⊥] Nacera Merahi,[⊥] Boris M. Emerit,[⊥] Alfredo Cagnotto,[§] Malgorzata Skorupska,[§] Tiziana Mennini,[§] and Julia C. Pinto[▽]

Dipartimento Farmaco Chimico Tecnologico, Università di Siena, Via Banchi di Sotto 55, 53100 Siena, Italy, Centro Interdipartimentale di Analisi e Determinazioni Strutturali, Università di Siena, via P.A. Mattioli 10, 53100 Siena, Italy, Institute of Pharmaceutical Chemistry, University of Innsbruck, Innrain 52A, A-6020 Innsbruck, Austria, Neurobiologie Cellulaire et Fonctionnelle, INSERM U. 288, Faculté de Médicine Pitié-Salpêtrière, 91, boulevard de l'Hôpital, 75634 Paris Cedex 13, France, Istituto di Ricerche Farmacologiche "M. Negri", Via Eritrea 62, 20157 Milano, Italy, and Laboratory of Medicinal Chemistry, NIDDK, Bethesda, Maryland 20892

Received January 12, 1995[⊗]

Synthesis and pharmacological evaluation of a series of condensed quinoline derivatives bearing a basic nitrogen on piperazine or [(dimethylamino)ethyl]thio moieties attached at the 2-position of the quinoline nucleus are described. 5-HT receptor binding studies revealed, for most of the compounds studied, nanomolar affinity for the 5-HT$_3$ receptor subtype. The most active compound, benzopyrano[3,4-*c*]quinoline derivative **5f**, displayed a K_i value very similar to that reported for quipazine along with an improved selectivity. Functional and *in vivo* testing carried out on three selected compounds showed that **5f,j,n** are potent 5-HT$_3$ receptor antagonists with potencies in the same range as the best known 5-HT$_3$ receptor antagonists ondansetron, tropisetron, and zacopride. The crystal and molecular structures of compounds **5f,j,n** were determined by single-crystal X-ray diffraction and used as starting structures for molecular modeling studies. Comparative molecular field analysis (CoMFA) was applied to binding constants of compounds **5a–p** and **6a–h**. The cross-validated r^2, derived from partial least-squares calculations, indicated a good predictive capacity for affinity values in the series of compounds investigated. Evidence for the prediction capacity is provided in the form of plots of actual vs predicted pK_i values. The steric and electrostatic features of the CoMFA-derived model are presented as standard coefficient contour maps of steric and electrostatic fields.

Introduction

Serotonin (5-hydroxytryptamine, 5-HT) exerts a wide variety of actions in man, which has led to demonstrate the existence of several 5-HT receptors to mediate them.[1] Indeed, four main classes of 5-HT receptors are at present well characterized (i.e., 5-HT$_1$, 5-HT$_2$, 5-HT$_3$, and 5-HT$_4$), and three novel receptor types were recently identified by cloning (5-HT$_5$, 5-HT$_6$, and 5-HT$_7$). Among them 5-HT$_1$ and 5-HT$_2$ classes were in turn subdivided in other subclasses,[2] while for 5-HT$_3$ receptors heterogeneity was questioned.[3] The majority of the 5-HT receptors belongs to the G-protein-linked receptor superfamily, involving in their action a second-messenger system such as cAMP or diacylglycerol and inositolphosphates. Indeed, only 5-HT$_3$ receptors are ligand-gated ion channel receptors.[1]

Recently a wide expansion was observed in the search for new 5-HT$_3$ receptor antagonists because of the great number of their potential applications in therapy. Ondansetron (**1**), the best known 5-HT$_3$ receptor antagonist, is on the market as an antiemetic agent to prevent the vomiting associated with anticancer chemotherapy. Furthermore, other possible therapeutic uses in anxiety, schizophrenia, drug abuse, and age-associated memory impairment are the subjects of intense investigations.[2,4] The great efforts made in this field led to the discovery of a number of potent and selective 5-HT$_3$ receptor antagonists which are now chemically classified into four main families as benzoates, benzamides, carbazolones, and indoles. Another class of 5-HT$_3$ antagonists which has not been as well studied as those mentioned above includes the arylpiperazines, namely (*m*-chlorophenyl)piperazine (**2**) and quipazine (**3**). These compounds which proved to behave as 5-HT$_3$ receptor antagonists are considered to be nonselective because they are able to interact with other 5-HT receptor subtypes.[1,3,5] This explains why quipazine, in spite of its high affinity for 5-HT$_3$ receptors, has not generally been used as a lead for the synthesis of more selective 5-HT$_3$ antagonists. However, in 1990, we started a research program[6] which led to the discovery of new quipazine derivatives with high affinity and selectivity for 5-HT$_3$ receptors.[7] Thus, modifications of the heteroaromatic portion of quipazine such as indeno fusion at the *c*-face yielded compounds **4** which showed high affinity and selectivity for 5-HT$_3$ receptors.[7] Moreover both the affinity and the selectiv-

[†] Centro Interdipartimentale di Analisi e Determinazioni Strutturali, Università di Siena.
[‡] Dipartimento Farmaco Chimica Techologico, Università di Siena.
[§] Istituto di Ricerche Farmacologiche "M. Negri".
[∥] University of Innsbruck.
[⊥] INSERM U. 288.
[▽] NIDDK.
[⊗] Abstract published in *Advance ACS Abstracts*, June 1, 1995.

0022-2623/95/1838-2692$09.00/0

Table 1. Preparative and Analytical Data of Compounds **5** and **6**

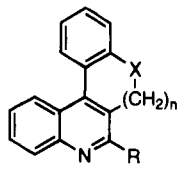

5

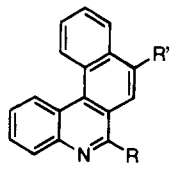

6

compd	X	*n*	R	R′	method	yield, %[a]	mp, °C (recr solv)[b]	formula	anal.[c]
5a	O	0	-N(C_2H_4)$_2$NH		A	84 (62)	>300 (E)	$C_{19}H_{17}N_3O$·2HCl·0.5H_2O	C,H,N
5b	O	0	-N(C_2H_4)$_2$N-CH_3		B	88	144–145 (H)	$C_{20}H_{19}N_3O$	C,H,N
5c	O	0	-N(C_2H_4)$_2$N-C_2H_5		B	88	145–146 (H)	$C_{21}H_{21}N_3O$	C,H,N
5d	O	0	-S(C_2H_4)N(CH_3)$_2$		C	71	115–116 (H)	$C_{19}H_{18}N_2OS$	C,H,N
5e	O	1	-N(C_2H_4)$_2$NH		A	85 (54)	>300 (E)	$C_{20}H_{19}N_3O$·2HCl	C,H,N
5f	O	1	-N(C_2H_4)$_2$N-CH_3		B	89	184–185 (H–C)	$C_{21}H_{21}N_3O$	C,H,N
5g	O	1	-N(C_2H_4)$_2$N-C_2H_5		B	75	143–144 (H–C)	$C_{22}H_{23}N_3O$	C,H,N
5h	O	1	-S(C_2H_4)N(CH_3)$_2$		C	78 (36)	235–236 (E–D)	$C_{20}H_{20}N_2OS$·HCl	C,H,N
5i	O	2	-N(C_2H_4)$_2$NH		A	97 (68)	>300 (E–D)	$C_{21}H_{21}N_3O$·HCl·0.25H_2O	C,H,N
5j[d]	O	2	-N(C_2H_4)$_2$N-CH_3						C,H,N
5k	O	2	-N(C_2H_4)$_2$N-C_2H_5		B	98	155–156 (H–C)	$C_{23}H_{25}N_3O$	C,H,N
5l	O	2	-S(C_2H_4)N(CH_3)$_2$		C	64 (53)	246–247 (E–D)	$C_{21}H_{22}N_2OS$·HCl	C,H,N
5m		2	-N(C_2H_4)$_2$NH		A	79 (55)	>300 (E–W)	$C_{21}H_{21}N_3$·2HCl·0.75H_2O	C,H,N
5n		2	-N(C_2H_4)$_2$N-CH_3		B	97	137–138 (H)	$C_{22}H_{23}N_3$	C,H,N
5o		2	-N(C_2H_4)$_2$N-C_2H_5		B	89 (62)	179–180 (E–D)	$C_{23}H_{25}N_3$·2HCl·0.75H_2O	C,H,N
5p		2	-S(C_2H_4)N(CH_3)$_2$		C	60 (35)	243–244 (E–D)	$C_{21}H_{22}N_2S$·HCl	C,H,N
6a			-N(C_2H_4)$_2$NH	H	A	75 (58)	>300 (E–D)	$C_{21}H_{19}N_3$·HCl·0.5H_2O	C,H,N
6b			-N(C_2H_4)$_2$N-CH_3	H	B	81	132–133 (H)	$C_{22}H_{21}N_3$	C,H,N
6c			-N(C_2H_4)$_2$N-C_2H_5	H	B	77	142–143 (H)	$C_{23}H_{23}N_3$	C,H,N
6d			-S(C_2H_4)N(CH_3)$_2$	H	C	69 (44)	236–237 (E–D)	$C_{21}H_{20}N_2S$·HCl	C,H,N
6e			-N(C_2H_4)$_2$NH	OCH_3	A	68 (47)	>300 (E–W)	$C_{22}H_{21}N_3O$·HCl	C,H,N
6f			-N(C_2H_4)$_2$N-CH_3	OCH_3	B	82	147–148 (H–C)	$C_{23}H_{23}N_3O$	C,H,N
6g			-N(C_2H_4)$_2$N-C_2H_5	OCH_3	B	90	129–130 (H)	$C_{24}H_{25}N_3O$	C,H,N
6h			-S(C_2H_4)N(CH_3)$_2$	OCH_3	C	81	79–80 (H)	$C_{22}H_{22}N_2OS$	C,H,N

[a] Values in parentheses are the yields as salt. [b] Recrystallization solvents: E, ethanol; H, *n*-hexane; C, cyclohexane; D, diethyl ether; W, water. [c] Analyses for the elements indicated are within ±0.4% of the theoretical values. [d] See ref 6c.

ity for 5-HT$_3$ sites of indenoquipazine derivatives **4** could be modulated by changes in the structure of the heteroaromatic portion.

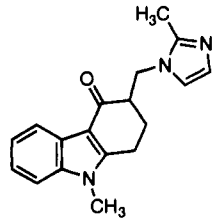

Ondansetron (1)

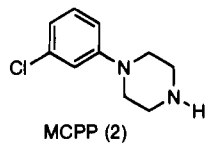

MCPP (2)

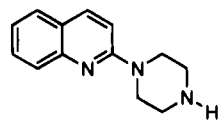

Quipazine (3)

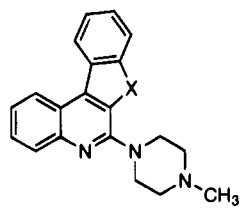

4a : X = C=O
4b : X = CH_2

We report now the synthesis and 5-HT receptor affinities of several condensed quipazine derivatives in the series **5** and **6**. The effects of different heteroaromatic portions on the binding to various 5-HT sites are discussed along with the effect of the replacement of the piperazine terminal nitrogen substituent as well as the replacement of the piperazine moiety with a [(dimethylamino)ethyl]thio chain. The *in vitro* and *in vivo* 5-HT$_3$ receptor antagonist activity of selected compounds was assessed by their ability to inhibit [^{14}C]guanidinium uptake in NG 108-15 hybrid cells[8] and antagonize the 5-HT-induced reflex bradycardia, the Bezold–Jarisch reflex, in the rat.[9] The 3D structure of the most representative compounds was studied by single-crystal X-ray diffraction or molecular mechanics. The data arising from the conformational analysis together with the structure–bioactivity data were used to build a predictive comparative molecular field analysis (CoMFA) model.

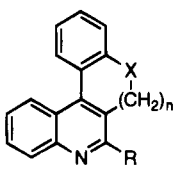

5
X = O, ·
n = 0, 1, 2

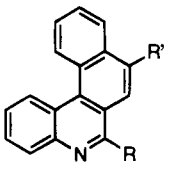

6
R′ = H, OCH_3

R = N(C_2H_4)$_2$N-H
N(C_2H_4)$_2$N-CH_3
N(C_2H_4)$_2$N-C_2H_5
S-C_2H_4-N(CH_3)$_2$

Chemistry

Compounds **5** and **6** (Table 1) were synthesized starting from the corresponding imino chlorides **7**–**12** as reported in Scheme 1. While in the synthesis of the unsubstituted piperazinyl derivatives **5a**,**e**,**i**,**m** and **6a**,**e**, the nucleophilic displacement of the chlorine atom by piperazine was carried out in ethylene glycol (method A); in the case of *N*-methylpiperazinyl derivatives **5b**,**f**,**n** and **6b**,**f** or *N*-ethylpiperazinyl derivatives **5c**,**g**,**k**,**o** and

Scheme 1

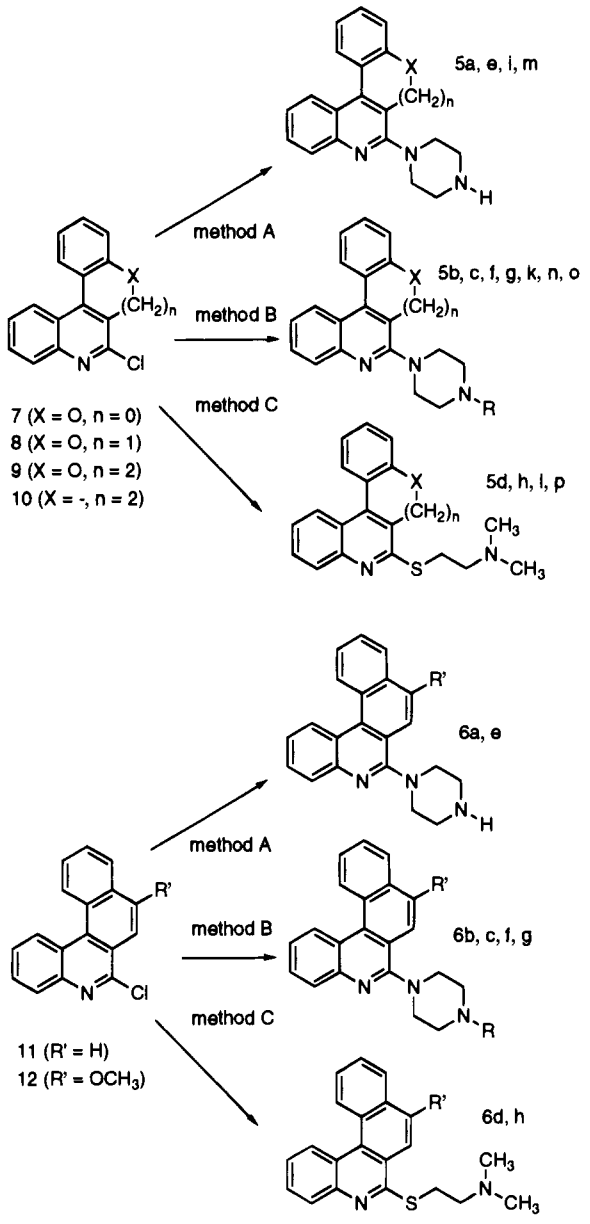

6c,**g**, the reaction was carried out without a solvent (method B). Treatment of imino chlorides **7**–**12** with 2-(dimethylamino)ethanethiolate, generated *in situ* following the procedure reported by Blackburn and co-workers,[10] gave the [2-(dimethylamino)ethyl]thio derivatives **5d**,**h**,**l**,**p** and **6d**,**h** (method C). Although imino chloride **7** is a known compound,[11] its synthesis was re-examined taking into account the chemistry developed by Walser and co-workers in the preparation of the benzofuro[2,3-*c*]quinoline ring system.[12]

The synthesis of **7**, according to our approach, is reported as depicted in Scheme 2. Chloroacetamide **14**, prepared by acylating benzophenone **13** with chloroacetyl chloride, was cyclized in the presence of potassium hydroxide in a dimethylformamide–water system to give hydroxyquinolone **15** and chloroquinolone **16** in a 1:2 ratio (approximately). After purification by chromatography, the undesired chloroquinolone **16** was separated allowing pure **15** to be recovered and cyclized by the nucleophilic displacement of the aromatic fluorine atom to afford benzofuroquinolinone **17** in satisfactory yield.[13] Compound **17** was promptly converted into its

Scheme 2[a]

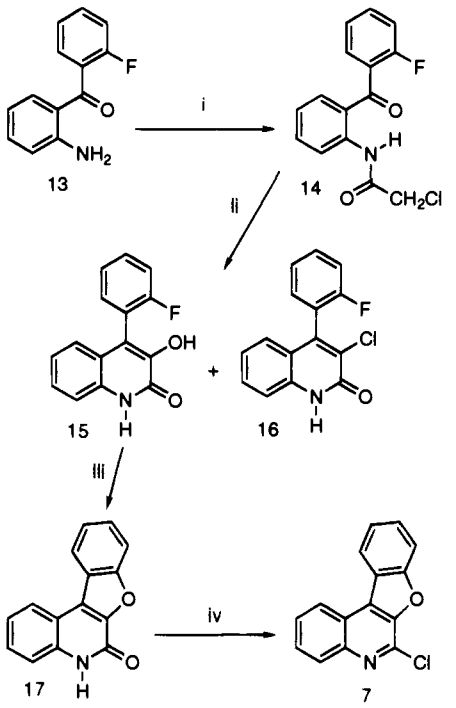

[a] Reagents: (i) $ClCH_2COCl$; CH_2Cl_2; (ii) KOH, DMF, H_2O; (iii) NaH, DMF; (iv) $POCl_3$.

Scheme 3[a]

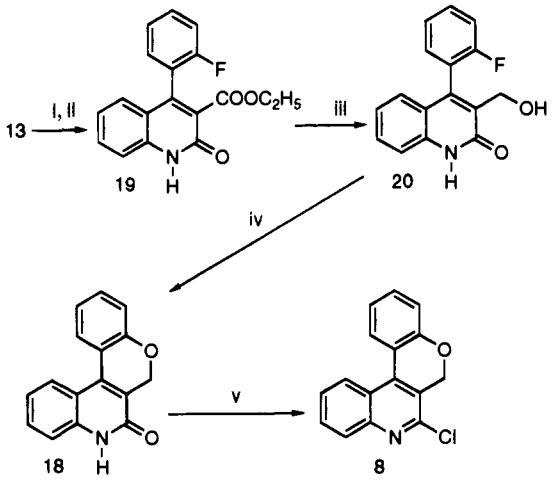

[a] Reagents: (i) $ClCOCH_2COOC_2H_5$, CH_2Cl_2; (ii) *t*-BuOK, EtOH; (iii) LAH, THF; (iv) NaH, DMF; (v) $POCl_3$.

corresponding imino chloride **7** with phosphorus oxychloride to reflux.

Imino chloride **8**, prepared starting from compound **18**, was easily obtained following the procedure reported by Walser et al.[14] for the synthesis of the 11-chloro derivative of **18** with slight modifications (Scheme 3). Benzophenone **13** was acylated with ethylmalonyl chloride and then cyclized with potassium *tert*-butoxide to give carbethoxyquinolone **19** in high yield. Lithium aluminum hydride reduction of **19** gave alcohol **20** which was cyclized by nucleophilic aromatic fluoride displacement into the expected benzopyranoquinolinone **18**.

Imino chlorides **9**–**11** are known compounds. While the synthesis of **9** has recently been reported by some of us,[6c] the preparation of **10** and **11** has been reinvestigated, and our approach is reported in Scheme 4. Cyclization of compound **21**[15] under the conditions of a typical Friedel–Crafts reaction gave a pale yellow, thick

Scheme 4[a]

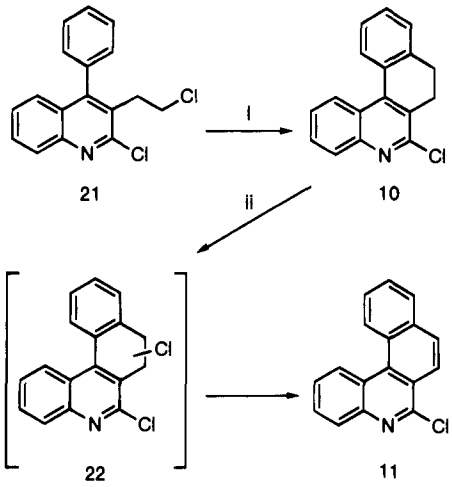

[a] Reagents: (i) $AlCl_3$, CH_2Cl_2; (ii) NCS, dibenzoyl peroxide, CCl_4.

Scheme 5[a]

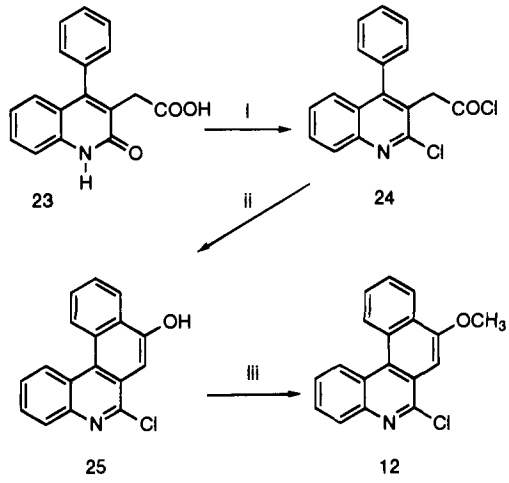

[a] Reagents: (i) $POCl_3$; (ii) $AlCl_3$, CH_2Cl_2; (iii) CH_3I, K_2CO_3, CH_3COCH_3.

oil which showed ^{1}H-NMR and MS in good agreement with structure **10**. Furthermore, it appeared to be pure at GC analysis. Since Paramasivam et al.[16] reported compound **10** melting at 80–81 or 95–96 °C, we synthesized it following the procedure they described and found the same physicochemical characteristics showed by compound **10** synthesized by Friedel–Crafts cyclization. Furthermore, the ^{1}H-NMR spectra of compound **10** synthesized through the two different procedures were in agreement with those reported in the literature.[16] Compound **11**[16b,17] was obtained starting from **10** by benzylic chlorination with *N*-chlorosuccinimide in the presence of dibenzoyl peroxide. An attempt to purify the crude reaction mixture by column chromatography gave directly **11**. Probably a spontaneous dehydrohalogenation of the unstable intermediate **22** occurred.

Finally, imino chloride **12** was prepared as outlined in Scheme 5. Quinolinoneacetic acid **23**[16a] was converted into the acid chloride **24** by stirring in phosphorus oxychloride to reflux and was promptly cyclized with anhydrous aluminum chloride into hydroxy benzophenanthridine **25**. The free hydroxy group of **25** was easily methylated with methyl iodide in the presence of potassium carbonate to give **12** in almost quantitative yield.

Computational Methods

The entire molecular modeling study was performed using the Sybyl 6.03 software package[18] running on a Silicon Graphics Indigo workstation. The molecules were either built starting from crystallographic coordinates (**5f,j,n**), derived from solid-state conformers of analogous compounds (**5e,g–i,k–m,o,p**), or assembled *de novo* from the Tripos standard fragment library (**5a–d**, **6a–h**). Hydrogen atoms were placed at standard bond distances and angles. Flexible side chains were set to a fully extended conformation. The potential energy of each structure was refined by a molecular mechanics procedure (MAXIMIN2) and an energy minimization procedure using the standard Tripos force field[19] until the root mean energy gradient was lower than 0.005 kcal/mol Å. Partial atomic charges were calculated using the method of Gasteiger and Marsili,[20] and coulomb terms were included in the potential energy minimization process.

CoMFA[21] was performed with the QSAR option of Sybyl. The requisite 3D grid was generated automatically by the software (2 Å grid spacing in x, y, and z directions, box size 19 × 22 × 13 Å, 840 points) assuring that every grid in all directions protruded at least 4 Å beyond the shape of each molecule. Steric and electrostatic interaction energies at lattice intersections were generated with a probe atom having the van der Waals properties of an sp^3 carbon and a charge of +1.0. The steric and electrostatic energy values were truncated at 30 kcal/mol. The electrostatic energy term was ignored at lattice intersections yielding maximal (30 kcal/mol) steric values. The linear expression of the CoMFA results was calculated with the partial least-squares analysis[22] (PLS) algorithm together with the cross-validation procedure. This method provides a determination of the optimal number of components and permits an evaluation of the predictivity of the model as indicated by the highest correlation (predictive r^2) value. PLS analysis of the descriptors without cross-validation afforded conventional r^2 values.

Results and Discussion

Qualitative Structure–Affinity Relationships. The aim of the present work was to assess whether the fusion at the *c*-face of quipazine with different bicyclic systems could lead to compounds with a selectivity for 5-HT$_3$ receptors higher than that reported for quipazine itself. Thus, the new compounds **5a–p** and **6a–h** were tested for binding on several 5-HT receptor subtypes (5-HT$_{1A}$, 5-HT$_{1B}$, 5-HT$_{2A}$, 5-HT$_{2C}$, and 5-HT$_3$) and 5-HT uptake in comparison with reference compounds using well-established protocols.[7,23] All the compounds showed a good affinity for 5-HT$_3$ serotonin receptors (Table 2). The most potent compounds (**5b,f,j,n**, and **6b**) were tested also on 5-HT$_4$ serotonin receptors.[24] Compound **5b** showed K_is for 5-HT$_4$ and 5-HT$_{2A}$ serotonin receptors respectively 550 and 36 times higher than for 5-HT$_3$ and is not active on the other serotonin receptor subtypes. Compound **5f** showed a K_i for 5-HT$_{2A}$ serotonin receptors 875 times higher than for 5-HT$_3$ and is inactive on other sites; also compounds **5j** and **6b** showed K_is for 5-HT$_{2A}$ serotonin receptors 630 and 97 times higher than for 5-HT$_3$ respectively. Compound **5n** showed K_is for 5-HT$_4$, 5-HT$_{2A}$, and 5-HT$_{2C}$ serotonin receptors 1886, 114, and 2057 times higher than for 5-HT$_3$. In Table 2,

Table 2. 5-HT Receptor Binding Profile of Compounds **5** and **6** (K_i (nM) ± SEM)[a]

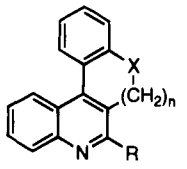

5

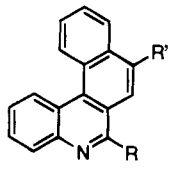

6

compd	X	n	R	R'	5-HT$_3$	5-HT$_4$	5-HT$_{2A}$	5-HT$_{2C}$	5-HT uptake	5-HT$_{1A}$	5-HT$_{1B}$
3					1.2[b]	NA[c]	130[d]		43[d]	1500[d]	208[e]
5a	O	0	-N(C_2H_4)$_2$NH		32.5 ± 14	NT[f]	1200 ± 200	NA	NA	NA	280 ± 55
5b	O	0	-N(C_2H_4)$_2$N-CH_3		12.5 ± 6.1	6900 ± 1100	450 ± 72	NA	NA	NA	NA
5c	O	0	-N(C_2H_4)$_2$N-C_2H_5		52.2 ± 15	NT	530 ± 79	NA	NA	NA	NA
5d	O	0	-S(C_2H_4)N(CH_3)$_2$		410 ± 190	NT	NA	NA	NA	NA	NA
5e	O	1	-N(C_2H_4)$_2$NH		11.5 ± 2.6	NT	2800 ± 740	NA	360 ± 100	NA	NA
5f	O	1	-N(C_2H_4)$_2$N-CH_3		1.6 ± 0.6	NA	1400 ± 320	NA	NA	NA	NA
5g	O	1	-N(C_2H_4)$_2$N-C_2H_5		53.3 ± 16	NT	1100 ± 210	NA	NA	NA	NA
5h	O	1	-S(C_2H_4)N(CH_3)$_2$		NA	NT	1800 ± 360	NA	NA	NA	NA
5i	O	2	-N(C_2H_4)$_2$NH		12.3 ± 3.2	NT	3200 ± 810	NA	330 ± 130	NA	420 ± 82
5j	O	2	-N(C_2H_4)$_2$N-CH_3		3.8 ± 1.2	NA	2400 ± 520	NA	NA	NA	NA
5k	O	2	-N(C_2H_4)$_2$N-C_2H_5		14.4 ± 3.1	NT	NA	NA	NA	NA	NA
5l	O	2	-S(C_2H_4)N(CH_3)$_2$		45.9 ± 19	NT	2800 ± 740	NA	NA	NA	1300 ± 150
5m		2	-N(C_2H_4)$_2$NH		5.4 ± 2.7	NT	640 ± 150	NA	2600 ± 670	NA	NA
5n		2	-N(C_2H_4)$_2$N-CH_3		3.5 ± 1.2	6600 ± 1000	400 ± 71	7200 ± 1700	NA	NA	NA
5o		2	-N(C_2H_4)$_2$N-C_2H_5		8.0 ± 1.6	NT	600 ± 80	NA	NA	NA	NA
5p		2	-S(C_2H_4)N(CH_3)$_2$		NA	NT	930 ± 310	NA	NT	NA	NA
6a			-N(C_2H_4)$_2$NH	H	130 ± 33	NT	1100 ± 240	NA	NA	NA	NA
6b			-N(C_2H_4)$_2$N-CH_3	H	9.5 ± 2.3	NA	920 ± 290	NA	NA	NA	NA
6c			-N(C_2H_4)$_2$N-C_2H_5	H	16.4 ± 11	NT	640 ± 130	NA	NA	NA	NA
6d			-S(C_2H_4)N(CH_3)$_2$	H	NA	NT	2400 ± 720	NA	NA	NA	NA
6e			-N(C_2H_4)$_2$NH	OCH_3	66.5 ± 27	NT	1100 ± 210	NA	NA	NA	NA
6f			-N(C_2H_4)$_2$N-CH_3	OCH_3	41.6 ± 15	NT	240 ± 18	2300 ± 410	NT	NA	NA
6g			-N(C_2H_4)$_2$N-C_2H_5	OCH_3	220 ± 35	NT	690 ± 96	NA	NT	NA	NA
6h			-S(C_2H_4)N(CH_3)$_2$	OCH_3	NA	NT	NA	NA	NA	NA	NA
5-HT					66 ± 8.3	230 ± 32				2.1 ± 0.1	2.5 ± 0.4
mesulergine								5.2 ± 0.8			
methysergide							1.6 ± 0.4				
indalpine									2.0 ± 0.1		
ondansetron					1.2 ± 0.2						

[a] Each value is the mean ± SEM of three determinations. [b] See ref 31. [c] NA: nonactive at 10 μM. [d] See ref 3. [e] See ref 5. [f] NT: not tested.

the results of the binding studies along with the binding profile reported in the literature for quipazine (**3**) (which is included for comparison) are summarized.

Most of the novel compounds inhibited [^{3}H]BRL43694 binding to 5-HT$_3$ receptors with K_i values in the nanomolar range, and their affinities for these receptors appeared to be affected by both the fused bicyclic system and the group incorporating the most basic nitrogen atom. Concerning the latter structural feature, it is clear that the piperazine nucleus stabilized the ligand–receptor complex better than the [(*N*,*N*-dimethylamino)-ethyl]thio side chain. In fact, all the compounds in which the most basic nitrogen atom was incorporated in the last group were only poorly active or inactive at 5-HT$_3$ receptors. Possible explanations of these findings might involve nonoptimal distance between the most basic nitrogen atom and the aromatic ring, lack of a second alkyl chain which contributes to the stabilization of the receptor–ligand complex, and the higher degree of conformational freedom of the noncyclic basic side chain.

When the [(dimethylamino)ethyl]thio moiety was replaced by piperazine as support of the most basic nitrogen, compounds **5** and **6** showed high affinity for 5-HT$_3$ receptors with K_is ranging from 1.6 (**5f**) to 220 (**6g**) nM. The substituent borne by the most basic nitrogen atom affected the ligand affinity for 5-HT$_3$ receptors to some extent, and as earlier observed,[7] the methyl group appeared to be optimal in the short series of substituents considered in the present work.

Concerning the large heteroaromatic portion of these complex arylpiperazines, it was assumed that a planar topography could facilitate the interaction with 5-HT$_3$ receptors.[7] In the design of the compounds reported herein, we intended to verify this assumption by synthesizing compounds with different geometries of the heteroaromatic portion (with planar and nonplanar topography). In Figure 1 the X-ray structures of compounds **5f**,**j**,**n** along with the 3D structures of compounds **5b** and **6b** built by molecular mechanics program Sybyl[18] are shown. In line with the above-mentioned hypothesis, planar compound **5b** was found to be active at 5-HT$_3$ receptors in the same nanomolar range as indenoquinolines **4** (**4a**, K_i = 3.0 nM; **4b**, K_i = 7.9 nM).[25] However, the nonplanar compound **5j** was also found to be active in the nanomolar range with a K_i value even 3-fold lower than that of planar **5b**. These data suggest that 5-HT$_3$ sites are able to accommodate both the planar and nonplanar heteroaromatic portions of these arylpiperazines. In light of this finding and comparing the 3D structures of compound **5j** and the 4-phenylquipazine derivative **26** (Figure 2), the difference observed in their affinity for 5-HT$_3$ receptors was rather surprising, **5j** being more potent by about 1 order of magnitude than the 4-phenylquipazine derivative **26** (K_i = 34 nM).[25] An explanation might possibly be found

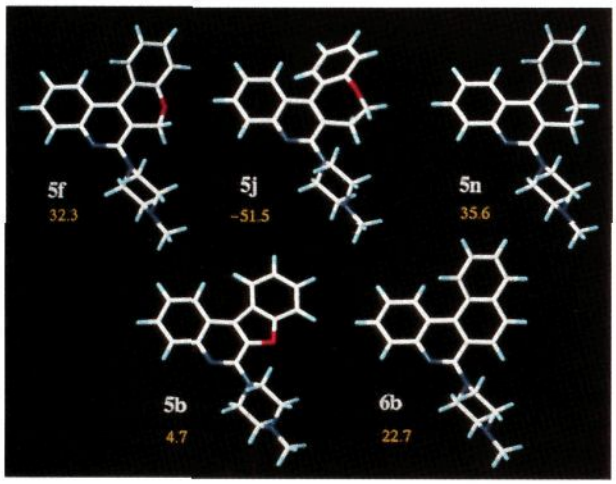

Figure 1. Structures of compounds **5f,j,n,b** and **6b**. Structures of compounds **5f,j,n** were built from crystallographic coordinates; structures of compounds **5b** and **6b** were built from the standard fragment library. Yellow captions: dihedral angle between the aromatic systems.

in the presumable different mobility of the phenyl ring in **5j** and **26**; thus, entropy could play an important role in determining the observed difference in the 5-HT$_3$ receptor affinity. However other parameters also, such as lipophilicity, could play an important role. Preliminary investigations on molecular dynamics[26] of compound **26** showed a freely rotating aromatic ring; molecular dynamics of compound **5j** compared with those of other members of this class of bioactive compounds is still under investigation, and further studies are required in order to understand the actual role of entropy.

The most potent compound to inhibit [^{3}H]BRL43694 binding appeared to be benzopyranoquinoline derivative **5f** which showed an affinity for 5-HT$_3$ receptors comparable with that of quipazine but with a markedly higher degree of selectivity. In fact, **5f** lacks affinity for 5-HT$_{1A}$, 5-HT$_{1B}$, and 5-HT$_{2C}$ receptors and the 5-HT uptake site, while it retains only a weak affinity for 5-HT$_{2A}$ receptors (Table 2). The selectivity ratios of this compound therefore appear to be much better than those calculated for quipazine (Table 3).

Table 3. Comparison between the Selectivity Ratios of **5f** and Quipazine (**3**) for 5-HT$_3$ versus Other 5-HT Receptor Subtypes[a]

compd	5-HT$_2$	5-HT uptake	5-HT$_{1A}$	5-HT$_{1B}$
5f	875	>6250	>6250	>6250
3	108	36	1250	173

[a] Each value is the ratio of the K_i value for the indicated site over that for 5-HT$_3$ receptors (from the data in Table 2).

Biological Activity. In addition to binding studies, two functional assays (see the Experimental Section) were carried out for assessing the potential agonist/antagonist activity of the compounds (**5f,j,n**) with the highest potencies as displacers of [^{3}H]BRL43694 specifically bound to 5-HT$_3$ receptors (see Table 2). Indeed, none of these compounds mimicked the effects of 5-HT on either the 5-HT$_3$ receptor-dependent accumulation of [^{14}C]guanidinium uptake in NG 108-15 hybridoma cells[8] (up to 10 μM in the assay medium) or the 5-HT$_3$ receptor-dependent Bezold–Jarisch reflex in urethane-anesthetized rats[9] (up to a dose of 120 μg/kg iv). Conversely, **5f,j,n** reversed in a concentration-dependent manner the stimulatory effect of 5-HT (in the presence of substance P, see ref 8) on [^{14}C]guanidinium uptake in NG 108-15 cells with IC$_{50}$ values of 16.9, 4.60, and 4.64 nM, respectively. (In Figure 3 are graphically represented the results obtained with compound **5j**.) These values are in the same range as those of well-characterized 5-HT$_3$ receptor antagonists such as ondansetron (IC$_{50}$ = 3.72 nM), tropisetron (IC$_{50}$ = 2.82 nM), and granisetron (IC$_{50}$ = 2.83 nM) indicating that the novel arylpiperazine derivatives acted as potent antagonits in this assay.

In agreement with the data obtained on NG 108-15 cells, investigations on urethane-anesthetized rats con-

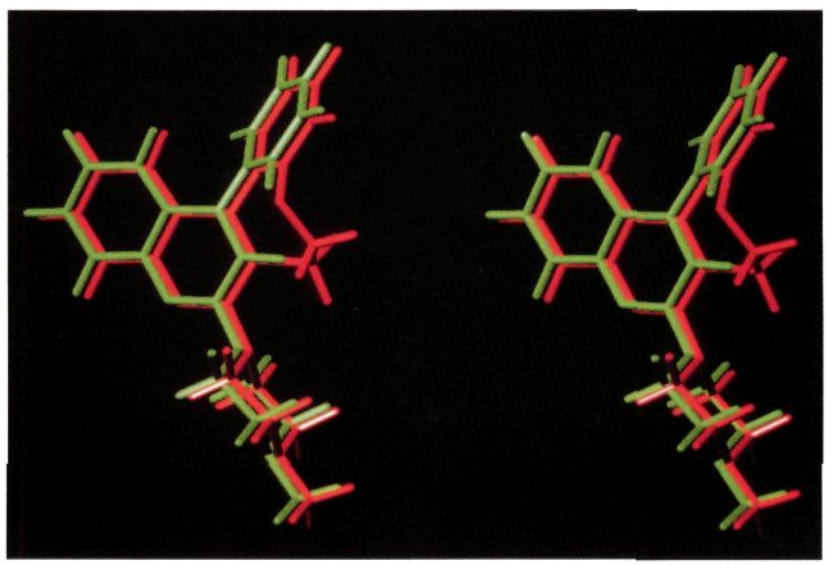

Figure 2. Relaxed stereoview of energy-minimized superimposed structures of compounds **5j** (red) and **26** (green). Compound **26** is 2-(4-methy-1-piperazinyl)-4-phenylquinoline.

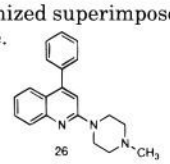

26

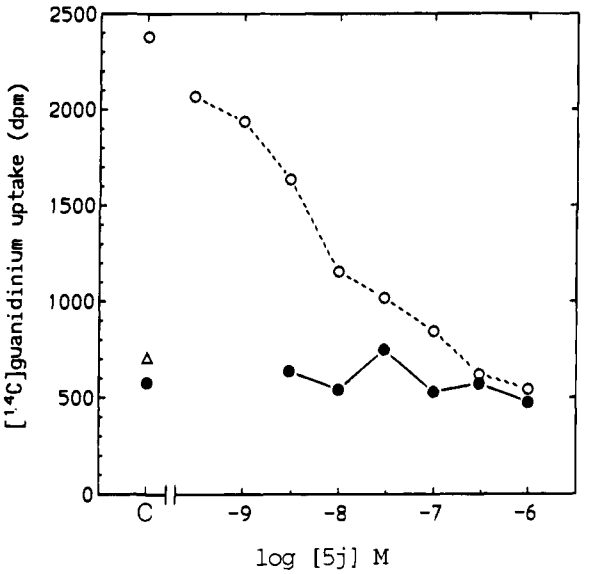

Figure 3. Concentration-dependent prevention by **5j** of 5-HT-stimulated [^{14}C]guanidinium uptake in NG 108-15 cells. △, basal uptake (without 5-HT and SP); •, with 10 μm SP alone; ○, with SP (10 μM) plus 5-HT (10 μM). Assays were carried out as described in the experimental part, and the accumulation of [^{14}C]guanidinium is expressed as dpm/culture dish. Each point is the mean of triplicate determinations with less than 5% variation among them.

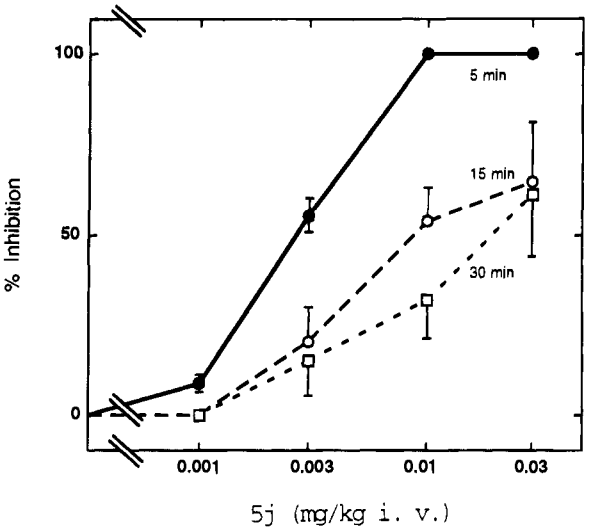

Figure 4. Dose-dependent inhibition by **5j** of 5-HT-evoked reflex bradycardia in urethane-anesthetized rats. Various doses of **5j** were injected 5, 15, or 30 min before the iv injection of 30 μg/kg 5-HT, and the amplitude of the 5-HT-evoked reflex bradycardia was compared to that observed in rats treated with the indoleamine alone. The reduction in the response to 5-HT is expressed as a percent of the maximal fall in heart rate observed in rats receiving 5-HT only. Each point is the mean ± SEM of three independent determinations.

firmed the 5-HT$_3$ receptor antagonist properties of compounds **5f,j,n**. Thus, complete blockade of the Bezold–Jarisch reflex elicited by a bolus iv injection of 5-HT (30 μg/kg) was observed 5 min after the iv administration of 120 μg/kg of either of these drugs. Dose–response curves indicated that half-maximal blockade of the reflex bradycardia due to 5-HT was obtained with 63 μg/kg **5f**, 3.04 μg/kg **5j**, or 1.10 μg/kg **5n** (iv) (means of two to three determinations) injected 5 min before the indoleamine. Significant reduction of the 5-HT-evoked bradycardia was still observed 30 min after the iv injection of 30 μg/kg iv of **5j** (~60%) or **5n** (~25%). (In Figure 4 are reported dose–response curves relating to compound **5j**.) In contrast, even at the highest dose tested, 120 μg/kg iv, **5f** did not affect 5-HT-induced bradycardia when injected 15 or 30 min before the agonist.

Studies of the effects of "classical" 5-HT$_3$ receptor antagonists in the same test indicated that half-maximal blockade of the reflex bradycardia due to 30 μg/kg iv 5-HT was obtained with 0.45 μg/kg iv zacopride, 3.05 μg/kg iv tropisetron, or 3.56 μg/kg iv ondansetron (means of three determinations) injected 5 min before the indoleamine. A marked reduction in the reflex bradycardia was still noted when zacopride or tropisetron was injected 30 min before the indoleamine. In contrast, the reflex bradycardia due to 30 μg/kg iv 5-HT was almost unaffected when ondansetron was injected 30 min before (~15% with 30 μg/kg iv antagonist), indicating a much shorter duration of action of the latter drug as compared to the other two 5-HT$_3$ antagonists.

In conclusion, novel quipazine derivatives appeared to act as potent and selective 5-HT$_3$ receptor antagonists. Among these compounds, **5j,n** were as potent and selective as ondansetron but had a longer duration of action than the latter 5-HT$_3$ receptor antagonist. In contrast to zacopride and tropisetron which also interact with the 5-HT$_4$ receptor,[27] **5j,n** were highly selective for 5-HT$_3$ receptors (see Table 2). Such comparisons suggest that **5j,n** should be of special interest for the selective *in vitro* and *in vivo* blockade of 5-HT$_3$ receptors. Their potential therapeutic value as antiemetic or psychotropic drugs is currently under investigation by means of appropriate preclinical tests.

Table 4. Statistical Results of CoMFA

Cross-validated Analysis

field offset (Å)				S_{Press}				
x	y	z	r^2_{cv}	comp1	comp2	comp3	comp4	comp5
0	0	0	0.701	0.650	0.753	0.809	0.795	0.776
1	0	0	0.705	0.646	0.736	0.832	0.854	0.843
1	1	0	0.718	0.631	0.773	0.816	0.854	0.843
1	1	1	0.697	0.654	0.760	0.802	0.804	0.886
−1	0	0	0.705	0.646	0.736	0.833	0.853	0.843
−1	−1	0	0.718	0.631	0.776	0.817	0.789	0.784
−1	−1	−1	0.697	0.654	0.758	0.805	0.806	0.884

Final Analysis without Cross-validation

s	0.492
r^2	0.829
F	106.600
prob of $r^2 = 0$	0.000

Comparative Molecular Field Analysis (CoMFA). In order to gain more insight into the quantitative structure–activity relationships (QSAR) of the compounds under study, we performed a 3D QSAR analysis using the CoMFA approach. The structures were aligned by rigid body least-squares rms fitting of all carbon and nitrogen atoms of the quinoline and piperazine moieties and subjected to CoMFA. In order to determine how well the model predicts data, each predictive value was cross-validated using initially five components resulting in a determination of the optimum number of components. The statistical evaluation is shown in Table 4. As can be seen from the results listed, use of one component is sufficient to obtain a satisfactory prediction. In order to determine the stability of

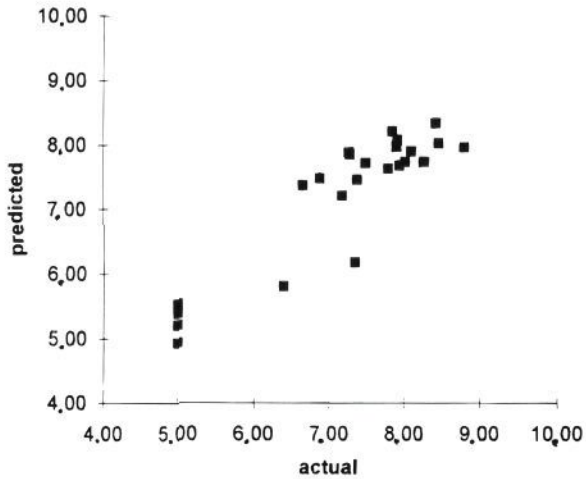

Figure 5. Plot of actual versus predicted binding affinities (pK_i values).

Table 5. Predicted Affinities (pK_i) and Residuals of Compounds **5a**–**p** and **6a**–**h** from Final CoMFA

compd	actual	calcd	resid	compd	actual	calcd	resid
5a	7.49	7.72	−0.23	**5m**	8.27	7.74	0.53
5b	7.90	7.97	−0.07	**5n**	8.46	8.02	0.44
5c	7.28	7.85	−0.57	**5o**	8.10	7.90	0.20
5d	6.39	5.81	0.58	**5p**	5.00	5.54	−0.54
5e	7.94	7.68	0.26	**6a**	6.88	7.48	−0.60
5f	8.80	7.96	0.84	**6b**	8.02	7.74	0.28
5g	7.27	7.88	−0.61	**6c**	7.79	7.64	0.15
5h	5.00	5.39	−0.39	**6d**	5.00	5.21	−0.21
5i	7.91	8.08	−0.17	**6e**	7.18	7.21	−0.03
5j	8.42	8.33	0.09	**6f**	7.38	7.46	−0.08
5k	7.84	8.21	−0.37	**6g**	6.65	7.37	−0.72
5l	7.34	6.18	1.16	**6h**	5.00	4.94	0.06

the model, the region was set to different offsets in x, y, and z directions, and a correlation analysis was done. All models exhibited a comparable predictivity. The final model obtained from the initial region using one component without cross-validation showed an r^2 value of 0.829 and a standard error of estimate of 0.492. Figure 5 shows a plot of the actual versus the predicted binding affinities (pK_i values); the results are listed in Table 5. The relative contribution of steric and electrostatic potential to the CoMFA regression equation for binding affinity to the 5-HT$_3$ receptor was found to be 57% and 43% steric and electrostatic, respectively. The standard deviation coefficient contour maps (Figures 6 and 7) derived from the final model display the 3D CoMFA contributions of steric and electrostatic potentials. These contour maps indicate where the changes in fields are correlated with changes in binding affinity.

From the steric interaction contour maps it can be deduced that the tolerated length of the side chain at N-4 of the piperazine moiety is limited. Additional steric interaction in this region would lead to a decreased binding affinity. A similar conclusion can be drawn for the length of the alkoxy side chain in compounds **6e**–**h**. On the other hand, substitution of the oxepine-fused phenyl ring in compounds **5i**,**j** at the 3- or 4-position with a positively polarized group could lead to compounds with enhanced affinity for the 5-HT$_3$ receptor, as can be deduced both from the steric and electrostatic contribution plots. We are aware that the predictive capacity of a 3D QSAR model strongly depends on the structural variability of compounds used for model construction. The molecules presented in this study exhibit a high degree of homology, and therefore a CoMFA derived from these compounds may not be predictive also for 5-HT$_3$ antagonists derived from other structural classes. Our model, however, may represent an effective tool for the design of new arylpiperazine compounds with pronounced 5-HT$_3$ affinity.

Conclusions

Starting from the high affinity and low selectivity showed by quipazine for 5-HT$_3$ receptors, this work has resulted in the discovery of some novel 5-HT$_3$ receptor

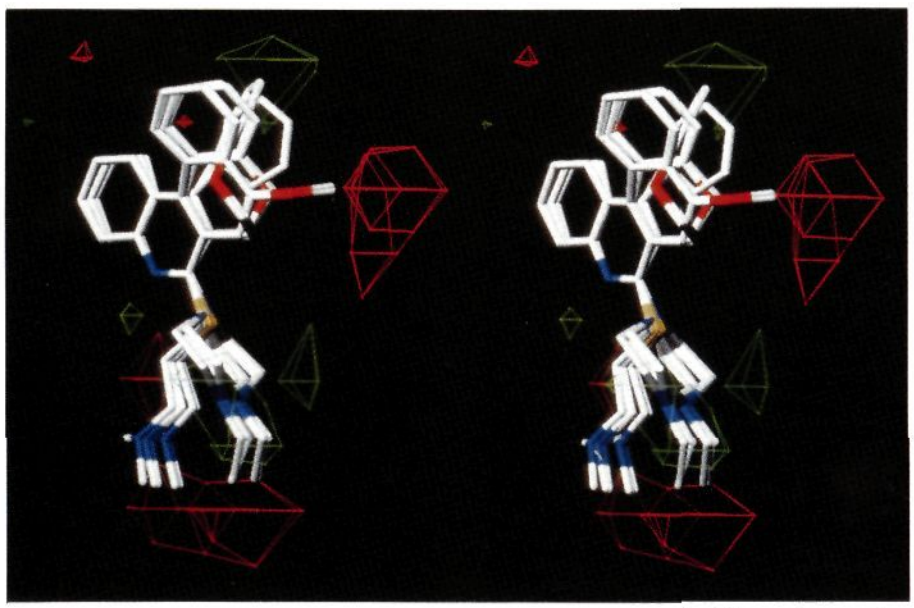

Figure 6. Relaxed stereoview of the CoMFA steric field graph for the 5-HT$_3$ model derived from the experimental data. Contour levels shown correspond with standard deviation × coefficient levels of 0.05 (green) and −0.004 (red). An increasing steric bulk in the green-coded (0.05) contour level would lead to higher target values (i.e., positive influence on affinity); additional steric bulk in the red-coded (−0.004) contour level negatively influences affinity.

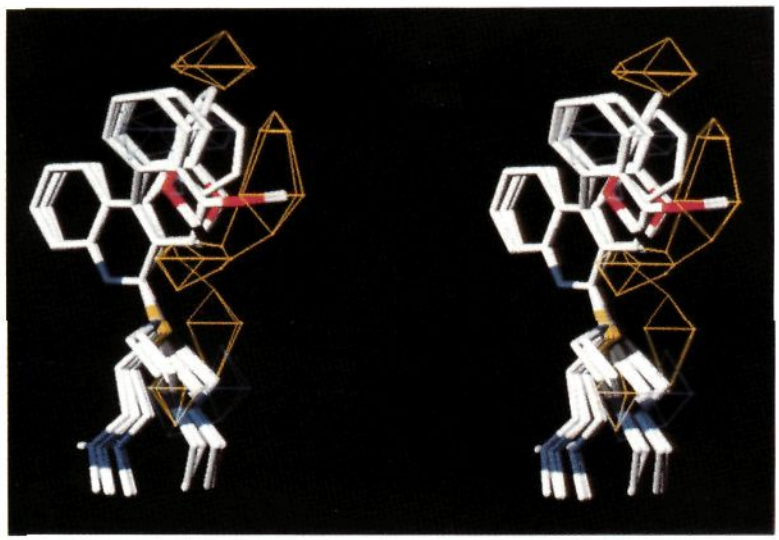

Figure 7. Relaxed stereoview of the CoMFA electrostatic field graph for the 5-HT_3 model derived from the experimental data. Contour levels shown correspond with standard deviation × coefficient levels of 0.05 (yellow) and −0.05 (blue). An increasing positive charge in the yellow-coded (0.05) contour level as well as additional negative charge in the blue-coded (−0.05) contour level would lead to higher target values (i.e., positively influence the affinity).

antagonists which, by virtue of their selectivity and potency, are interesting candidates for preclinical tests as antiemetic or psychotropic drugs. The present study demonstrates the usefulness of the "ring-fused analogue" concept in inducing selectivity in nonselective mother compounds. Furthermore, the CoMFA model developed during these investigations appears to be an interesting tool for the design of new, potent 5-HT_3 ligands based on the arylpiperazine skeleton. Finally, the observed shift between the agonistic properties described for quipazine in guanidinium accumulation[8] and the antagonistic properties of the ring-fused quipazine analogues here described provides an interesting topic for new investigations.

Experimental Section

Melting points were determined in open capillaries on a Büchi 510 apparatus and are uncorrected. Microanalyses were carried out using a Perkin-Elmer 240C elemental analyzer. Merck silica gel 60, 70−230 mesh, was used for column chromatography, and Riedel-de Haen DC-Mikrokarten SI F 37341 were used for TLC. Infrared spectra (IR) were recorded in Nujol mulls with a Perkin-Elmer model 397 spectrophotometer. ^{1}H-NMR spectra were recorded with a Bruker AC 200 spectrometer in the indicated solvents (TMS as internal standard); the values of chemical shifts are expressed in ppm and coupling constants (J) in hertz (Hz). Mass spectra (EI, 70 eV) were recorded on a VG 70-250S spectrometer. IR, NMR spectra, and elemental analyses were performed by the Dipartimento Farmaco Chimico Tecnologico, Università di Siena. Mass spectra were performed by Centro di Analisi e Determinazioni Strutturali, Università di Siena.

General Procedures for the Synthesis of Compounds **5** and **6**. Method A. A mixture of the appropriate imino chloride **7**−**12** (1.0 mmol) in ethylene glycol (30 mL) and piperazine (3.0 g, 34.8 mmol) was heated at 130−140 °C under nitrogen for a suitable time (2−23 h), and the reaction course was followed by TLC. When the chloro derivative disappeared from the chromatogram, the reaction mixture was poured into ice−water (300 mL) and extracted with chloroform (3 × 20 mL). The organic layer was thoroughly washed with water (5 × 15 mL), dried over sodium sulfate, and concentrated *in vacuo* to give a residue which was purified by column chromatography. Elution with ethyl acetate−triethylamine−ethanol (6:2:2) yielded pure piperazinyl derivatives **5a**,**e**,**i**,**m** and **6a**,**e**. The free bases were converted into the corresponding hydrochloride salts according to Blackburn et al.[10] Finally, salts were recrystallized from the suitable solvents.

6-(1-Piperazinyl)benzofuro[2,3-*c*]quinoline dihydrochloride (5a): ^{1}H-NMR (DMSO-d_6) 3.40 (br s, 4H), 4.28 (br s, 4H), 7.57−7.81 (m, 5H), 7.97 (d, J = 8.3, 1H), 8.64-8.73 (m, 2H), 9.35 (br s, 2H).

7-(1-Piperazinyl)-6*H*-[1]benzopyrano[3,4-*c*]quinoline dihydrochloride (5e): ^{1}H-NMR (DMSO-d_6) 3.35 (br s, 4H), 3.52 (br s, 4H), 5.15 (s, 2H), 7.25−7.37 (m, 2H), 7.48−7.61 (m, 2H), 7.77 (t, J = 7.1, 1H), 7.97 (d, J = 7.8, 1H), 8.12 (d, J = 7.8, 1H), 8.43 (d, J = 8.4, 1H), 9.36 (br s, 2H).

6,7-Dihydro-8-(1-piperazinyl)[1]benzoxepino[4,5-*c*]quinoline hydrochloride (5i): ^{1}H-NMR (DMSO-d_6) 2.59−2.77 (m, 1H), 3.08−3.16 (m, 1H), 3.39 (br s, 4H), 3.47 (brs, 4H), 4.50−4.63 (m, 2H), 7.31−7.61 (m, 5H), 7.68−7.75 (m, 1H), 7.84−7.95 (m, 2H), 9.26 (br s, 2H); MS m/z 331 (M^+, 14).

7,8-Dihydro-6-(1-piperazinyl)benzo[*k*]phenanthridine dihydrochloride (5m): ^{1}H-NMR (DMSO-d_6) 2.72−2.91 (pair of multiplet, 4H), 3.34 (br s, 4H), 3.59 (br s, 4H), 7.46−7.56 (m, 4H), 7.68−7.77 (m, 1H), 7.88−7.96 (m, 2H), 8.33 (d, J = 8.4, 1H), 9.24 (br s, 2H).

6-(1-Piperazinyl)benzo[*k*]phenanthridine hydrochloride (6a): ^{1}H-NMR (DMSO-d_6) 3.45 (br s, 4H), 3.70 (br s, 4H), 7.63−7.89 (m, 4H), 8.03−8.28 (m, 4H), 8.96 (d, J = 8.3, 1H), 9.09−9.14 (m, 1H), 9.37 (br s, 2H).

8-Methoxy-6-(1-piperazinyl)benzo[*k*]phenanthridine hydrochloride (6e): ^{1}H-NMR (DMSO-d_6) 3.45 (br s, 4H), 3.69 (br s, 4H), 4.22 (s, 3H), 7.45 (s, 1H), 7.63−7.72 (m, 2H), 7.76−7.90 (m, 2H), 8.00 (d, J = 7.8, 1H), 8.46−8.50 (m, 1H), 8.86 (d, J = 7.9, 1H), 9.07−9.11 (m, 1H), 9.37 (br s, 2H); MS m/z 343 (M^+, 23).

Method B. A solution of the appropriate imino chloride **7**−**12** (1.0 mmol) in *N*-methylpiperazine or *N*-ethylpiperazine (8 mL) was heated at 120−130 °C under nitrogen for a suitable time (2−24 h), and the reaction course was followed by TLC. When the chloro derivative disappeared from the chromatogram, the reaction mixture was poured into ice−water (250 mL) and extracted with chloroform (3 × 20 mL). The organic layer was washed with water (2 × 30 mL), dried over sodium sulfate, and concentrated under reduced pressure. Chromatographic purification of the residue with ethyl acetate−triethylamine (8:2) as the eluent gave pure piperazinyl derivatives **5b**,**c**,**f**,**g**,**k**,**n**,**o** and **6b**,**c**,**f**,**g**. The free bases were crystallized from the suitable solvents or converted into the corresponding hydrochloride salts by a reported procedure,[10] and then the salts were recrystallized.

6-(4-Methyl-1-piperazinyl)benzofuro[2,3-*c*]quinoline (5b): ^{1}H-NMR ($CDCl_3$) 2.62 (s, 3H), 3.01 (br s, 4H), 4.35 (br s, 4H), 7.47–7.75 (m, 5H), 7.94 (d, J = 8.3, 1H), 8.38–8.44 (m, 2H).

6-(4-Ethyl-1-piperazinyl)benzofuro[2,3-*c*]quinoline (5c): ^{1}H-NMR ($CDCl_3$) 1.23 (t, J = 7.3, 3H), 2.61 (q, J = 7.2, 2H), 2.80 (t, J = 4.9, 4H), 4.20 (t, J = 4.9, 4H), 7.43–7.73 (m, 5H), 7.93 (d, J = 8.3, 1H), 8.37–8.42 (m, 2H).

7-(4-Methyl-1-piperazinyl)-6*H*-[1]benzopyrano[3,4-*c*]quinoline (5f): ^{1}H-NMR ($CDCl_3$) 2.41 (s, 3H), 2.66 (t, J = 4.7, 4H), 3.34 (t, J = 4.8, 4H), 5.05 (s, 2H), 7.16–7.26 (m, 2H), 7.35–7.44 (m, 2H), 7.62 (t, J = 7.0, 1H), 7.92–8.06 (m, 2H), 8.39 (d, J = 8.7, 1H).

7-(4-Ethyl-1-piperazinyl)-6*H*-[1]benzopyrano[3,4-*c*]quinoline (5g): ^{1}H-NMR ($CDCl_3$) 1.16 (t, J = 7.0, 3H), 2.54 (q, J = 7.2, 2H), 2.68 (t, J = 4.5, 4H), 3.34 (t, J = 4.8, 4H), 5.05 (s, 2H), 7.16–7.26 (m, 2H), 7.34–7.44 (m, 2H), 7.56–7.67 (m, 1H), 7.92–8.05 (m, 2H), 8.38 (d, J = 8.1, 1H).

6,7-Dihydro-8-(4-ethyl-1-piperazinyl)[1]benzoxepino[4,5-*c*]quinoline (5k): ^{1}H-NMR ($CDCl_3$) 1.19 (t, J = 7.3, 3H), 2.59 (q, J = 7.2, 2H), 2.68–2.85 (m, 5H), 3.07–3.15 (m, 1H), 3.42 (t, J = 4.0, 4H), 4.55–4.60 (m, 2H), 7.24–7.63 (m, 6H), 7.85–7.95 (m, 2H); MS m/z 359 (M^+, 9).

7,8-Dihydro-6-(4-methyl-1-piperazinyl)benzo[*k*]phenanthridine (5n): ^{1}H-NMR ($CDCl_3$) 2.39 (s, 3H), 2.64 (t, J = 4.7, 4H), 2.70–2.87 (pair of multiplet, 4H), 3.40 (t, J = 4.7, 4H), 7.31–7.44 (m, 4H), 7.54–7.62 (m, 1H), 7.88–7.95 (m, 2H), 8.33 (d, J = 7.8, 1H).

7,8-Dihydro-6-(4-ethyl-1-piperazinyl)benzo[*k*]phenanthridine dihydrochloride (5o): ^{1}H-NMR (DMSO-d_6) 1.36 (t, J = 7.2, 3H), 2.81–2.92 (pair of multiplet, 4H), 3.16–3.40 (m, 4H), 3.59–3.78 (m, 4H), 4.02 (d, J = 13.6, 2H), 7.48–7.63 (m, 4H), 7.77–7.93 (m, 2H), 8.24 (d, J = 8.3, 1H), 8.34 (d, J = 8.3, 1H), 11.57 (br s, 1H).

6-(4-Methyl-1-piperazinyl)benzo[*k*]phenanthridine (6b): ^{1}H-NMR ($CDCl_3$) 2.44 (s, 3H), 2.75 (t, J = 4.6, 4H), 3.58 (t, J = 4.7, 4H), 7.50–7.73 (m, 4H), 7.88 (d, J = 8.8, 1H), 8.00–8.15 (m, 3H), 8.88 (d, J = 8.4, 1H), 9.06–9.10 (m, 1H).

6-(4-Ethyl-1-piperazinyl)benzo[*k*]phenanthridine (6c): ^{1}H-NMR ($CDCl_3$) 1.18 (t, J = 7.3, 3H), 2.57 (q, J = 7.2, 2H), 2.77 (t, J = 4.8, 4H), 3.58 (t, J = 4.8, 4H), 7.50–7.72 (m, 4H), 7.87 (d, J = 8.8, 1H), 8.00–8.16 (m, 3H), 8.88 (d, J = 8.3, 1H), 9.06–9.10 (m, 1H).

6-(4-Methyl-1-piperazinyl)-8-methoxybenzo[*k*]phenanthridine (6f): ^{1}H-NMR ($CDCl_3$) 2.44 (s, 3H), 2.75 (t, J = 4.4, 4H), 3.56 (t, J = 4.5, 4H), 4.14 (s, 3H), 7.43–7.74 (m, 5H), 8.03 (d, J = 7.6, 1H), 8.45–8.50 (m, 1H), 8.80 (d, J = 8.2, 1H), 9.02–9.07 (m, 1H).

6-(4-Ethyl-1-piperazinyl)-8-methoxybenzo[*k*]phenanthridine (6g): ^{1}H-NMR ($CDCl_3$) 1.18 (t, J = 7.3, 3H), 2.57 (q, J = 7.1, 2H), 2.78 (t, J = 4.2, 4H), 3.58 (br s, 4H), 4.14 (s, 3H), 7.43–7.74 (m, 5H), 8.04 (d, J = 7.6, 1H), 8.45–8.50 (m, 1H), 8.80 (d, J = 8.1, 1H), 9.02–9.07 (m, 1H).

Method C. To a stirred suspension of sodium hydride (0.053 g, 2.2 mmol) in dry DMF (5 mL) at 0–5 °C was added 2-(dimethylamino)ethanethiol hydrochloride (0.156 g, 1.1 mmol) over 25 min. The mixture was allowed to warm to room temperature and stirred for 1 h. A solution of the suitable imino chloride **7–12** (1.0 mmol) in dry DMF (10 mL) was added, and the resulting mixture was heated at 75–85 °C under nitrogen for an appropriate time (1–5 h). The reaction course was followed by TLC. When the imino chloride disappeared from the chromatogram, the cooled reaction mixture was poured into ice–water (300 mL). The precipitate was extracted with chloroform (4 × 15 mL), and the combined extracts were thoroughly washed with water (5 × 20 mL), dried over sodium sulfate, and evaporated under reduced pressure. Chromatographic purification of the residue with ethyl acetate–triethylamine (8:2) as the eluent gave the expected [(dimethylamino)ethyl]thio derivative which was recrystallized from the suitable solvent (**5d** and **6h**) or converted into the hydrochloric salt by a reported procedure[10] and then recrystallized (**5h**,**l**,**p** and **6d**).

6-[[2-(*N*,*N*-Dimethylamino)ethyl]thio]benzofuro[2,3-*c*]quinoline (5d): ^{1}H-NMR ($CDCl_3$) 2.80 (s, 6H), 3.22–3.29 (m, 2H), 3.91 (t, J = 7.8, 2H), 7.50–7.81 (m, 5H), 8.09-8.13 (m, 1H), 8.38–8.52 (m, 2H).

7-[[2-(*N*,*N*-Dimethylamino)ethyl]thio]-6*H*-[1]benzopyrano[3,4-*c*]quinoline hydrochloride (5h): ^{1}H-NMR (DMSO-d_6) 2.93 (s, 6H), 3.42–3.49 (m, 2H), 3.76–3.84 (m, 2H), 5.17 (s, 2H), 7.25–7.36 (m, 2H), 7.54 (t, J = 7.8, 1H), 7.64–7.72 (m, 1H), 7.85 (t, J = 7.3, 1H), 8.11–8.16 (m, 2H), 8.49 (d, J = 8.4, 1H), 10.70 (br s, 1H).

6,7-Dihydro-8-[[2-(*N*,*N*-dimethylamino)ethyl]thio][1]benzoxepino[4,5-*c*]quinoline hydrochloride (5l): ^{1}H-NMR (DMSO-d_6) 2.69–2.85 (m, 1H), 2.95 (s, 6H), 3.00–3.09 (m, 1H), 3.42–3.50 (m, 2H), 3.74–3.82 (m, 2H) 4.40–4.62 (m, 2H), 7.32–7.65 (m, 5H), 7.80 (t, J = 7.2, 1H), 7.95 (d, J = 8.3, 1H), 8.13 (d, J = 8.2, 1H), 10.81 (br s, 1H); MS m/z 350 (M^+, 2).

7,8-Dihydro-6-[[2-(*N*,*N*-dimethylamino)ethyl]thio]benzo[*k*]phenanthridine dihydrochloride (5p): ^{1}H-NMR (DMSO-d_6) 2.81–2.93 (m, 4H), 2.95 (s, 6H), 3.41–3.49 (m, 2H), 3.71–3.79 (m, 2H), 7.46–7.66 (m, 4H), 7.79 (t, J = 7.2, 1H), 7.92–7.97 (m, 1H), 8.09 (d, J = 7.8, 1H), 8.39 (d, J = 8.3, 1H), 10.49 (br s, 1H).

6-[[2-(*N*,*N*-Dimethylamino)ethyl]thio]benzo[*k*]phenanthridine hydrochloride (6d): ^{1}H-NMR (DMSO-d_6) 2.98 (s, 6H), 3.50–3.57 (m, 2H), 3.83–3.91 (m, 2H), 7.75–7.95 (m, 4H), 8.19–8.31 (m, 4H), 9.04 (d, J = 8.1, 1H), 9.16–9.21 (m, 1H), 10.26 (br s, 1H).

6-[[2-(*N*,*N*-Dimethylamino)ethyl]thio]-8-methoxybenzo[*k*]phenanthridine (6h): ^{1}H-NMR ($CDCl_3$) 2.43 (s, 6H), 2.82 (t, J = 7.2, 2H), 3.69 (t, J = 7.3, 2H), 4.17 (s, 3H), 7.46 (s, 1H), 7.52–7.75 (m, 4H), 8.06–8.11 (m, 1H), 8.48–8.52 (m, 1H), 8.84 (d, J = 8.3, 1H), 9.06–9.10 (m, 1H).

2-Chloro-2′-(2-fluorobenzoyl)acetanilide (14). To a solution of 13 (4.3 g, 0.02 mol) in dichloromethane (100 mL) at 0 °C was added chloroacetyl chloride (1.7 mL, 0.022 mol) dropwise, and the reaction mixture was stirred at room temperature for 1 h. Afterward a saturated sodium bicarbonate solution (40 mL) was added at 0–5 °C with vigorous stirring, and the organic layer was separated, dried over sodium sulfate, and concentrated under reduced pressure. Pure **14** (5.8 g, 99%) was obtained as a white solid. Recrystallization from cyclohexane gave an analytical sample melting at 120–122 °C: IR 3180, 1680, 1640 cm^{-1}; ^{1}H-NMR ($CDCl_3$) 4.23 (s, 2H), 7.10–7.31 (m, 3H), 7.47–7.65 (m, 4H), 8.73 (d, J = 8.6, 1H), 12.09 (br s, 1H). Anal. ($C_{15}H_{11}NO_2ClF$) C, H, N.

4-(2-Fluorophenyl)-3-hydroxy-2(1*H*)-quinolinone (15). To a solution of **14** (2.0 g, 6.86 mmol) in DMF (40 mL) with 85% KOH (3.0 g, 45.4 mmol) was added water (15 mL). The reaction mixture was stirred at room temperature for 1.5 h, diluted with ice–water (250 mL), and made acid with 3 N hydrochloric acid. The precipitate was collected by filtration, washed with water, dried, and purified by column chromatography with chloroform–ethyl acetate (9:1) and then chloroform–ethyl acetate (7:3) as successive eluents, giving **15** as a white solid (0.44 g, 25%). An analytical sample recrystallized from benzene–ethyl acetate melted at 255–256 °C: IR 3400, 3150, 1650, 1630 cm^{-1}; ^{1}H-NMR (DMSO-d_6) 6.97 (d, J = 8.2, 1H), 7.08–7.16 (m, 1H), 7.32–7.61 (m, 6H), 9.49 (s, 1H), 12.27 (br s, 1H); MS m/z 255 (M^+, 84). Anal. ($C_{15}H_{10}NO_2F$) C, H, N.

3-Chloro-4-(2-fluorophenyl)-2(1*H*)-quinolinone (16). Compound **16** was isolated from the chloroform–ethyl acetate (9:1) fraction of the above-cited purification by column chromatography (0.8 g, 43%). Recrystallization from ethanol–ethyl acetate gave an analytical sample melting at 269–272 °C: IR 3280, 1670 cm^{-1}; ^{1}H-NMR (DMSO-d_6) 6.98 (d, J = 8.4, 1H), 7.15–7.24 (m, 1H), 7.41–7.72 (m, 6H), 12.53 (br s, 1H); MS m/z 273 (M^+, 100). Anal. ($C_{15}H_9NOClF$) C, H, N.

Benzofuro[2,3-*c*]quinolin-6(5*H*)-one (17). A mixture of **15** (0.4 g, 1.6 mmol) in dry DMF (10 mL) with sodium hydride (0.12 g, 4.8 mmol) was refluxed for 5 h under nitrogen and then poured into ice–water (200 mL). The aqueous mixture was made acidic with 3 N HCl, and the precipitate was collected by filtration, washed with water, and dried. Pure **17** (0.32 g, 87%) was obtained by washing the crude product with hot ethyl acetate. Recrystallization from ethanol–DMF gave an analytical sample melting at 351 °C dec (lit.[11] mp 322–324 °C): IR 3160, 1680 cm^{-1}; ^{1}H-NMR (DMSO-d_6) 7.40–7.77

(m, 5H), 7.95 (d, J = 8.2, 1H), 8.51 (d, J = 8.0, 1H), 8.63 (d, J = 7.6, 1H), 12.27 (br s, 1H); MS m/z 235 (M^+, 100). Anal. ($C_{15}H_9NO_2$) C, H, N.

6-Chlorobenzofuro[2,3-*c*]quinoline (7). A mixture of **17** (0.4 g, 1.7 mmol) in $POCl_3$ (6 mL, 64.4 mmol) was refluxed for 1 h and then poured onto crushed ice. The precipitate was extracted with dichloromethane (3 × 20 mL), and the combined extracts were washed with brine, dried over sodium sulfate, and concentrated under reduced pressure. The residue was purified by column chromatography using dichloromethane as eluent, and pure **7** was obtained (0.38 g, 88%) as a white solid. An analytical sample recrystallyzed from cyclohexane melted at 154–155 °C (lit.[11] mp 157.5–158.5 °C): ^{1}H-NMR ($CDCl_3$) 7.49–7.79 (m, 5H), 8.13–8.28 (m, 1H), 8.32 (d, J = 7.8, 1H), 8.42–8.47 (m, 1H); MS m/z 253 (M^+, 100). Anal. ($C_{15}H_8NOCl$) C, H, N.

Ethyl 4-(2-Fluorophenyl)-2(1*H*)-oxoquinoline-3-carboxylate (19). To a solution of 13 (4.3 g, 0.02 mol) in dichloromethane (50 mL) was added carbethoxyacetyl chloride (3.1 mL, 0.024 mol) at 0 °C. After 20 min, a saturated sodium bicarbonate solution (40 mL) was added at 0–5 °C with vigorous stirring. The organic layer was separated, dried over sodium sulfate, and concentrated under reduced pressure. The residue was dissolved in absolute ethanol (100 mL), and potassium *tert*-butoxide (1.0 g, 8.91 mmol) was added. The reaction mixture was stirred at room temperature for 1 h and then diluted with water and made acidic with 3 N HCl. The precipitate was collected by filtration, washed with water and then with ethyl acetate, and dried to give **19** as white crystals (4.3 g, 69%). An analytical sample recrystallized from ethyl acetate melted at 186–187 °C: IR 3160, 1730, 1650 cm^{-1}; ^{1}H-NMR ($CDCl_3$) 1.00 (t, J = 7.0, 3H), 4.10–4.21 (m, 2H), 7.14–7.34 (m, 5H), 7.44–7.55 (m, 3H), 12.65 (br s, 1H). Anal. ($C_{18}H_{14}NO_3F$) C, H, N.

4-(2-Fluorophenyl)-3-(hydroxymethyl)quinolin-2(1*H*)-one (20). To a suspension of lithium aluminum hydride (1.0 g, 26.4 mmol) in dry THF (10 mL) was slowly added a solution of **19** (1.6 g, 5.14 mmol) at −20 °C. After stirring for 30 min at −20–0 °C, the hydride was hydrolyzed by addition of water (5 mL) and the mixture was partitioned between chloroform and 3 N HCl. The organic layer was washed with water, dried over sodium sulfate, and concentrated under reduced pressure. The residue was crystallized from ethyl acetate–ethanol to give **20** (1.1 g, 79%; mp 225–226 °C): IR 3290, 3160, 1650 cm^{-1}; ^{1}H-NMR (DMSO-d_6) 4.18 (ABq, J = 11.1, 2H), 4.65 (br s, 1H), 6.93 (d, J = 8.0, 1H), 7.13 (t, J = 7.3, 1H), 7.38–7.68 (m, 6H), 12.07 (br s, 1H). Anal. ($C_{16}H_{12}NO_2F$) C, H, N.

6,8-Dihydro-7*H*-[1]benzopyrano[3,4-*c*]quinolin-7-one (18). To a solution of **20** (0.8 g, 2.97 mmol) in dry DMF (10 mL) was added sodium hydride (0.22 g, 9.17 mmol), and the mixture was heated at 135–140 °C under nitrogen for 15 min. The cooled reaction mixture was then poured into ice–water (250 mL). The aqueous mixture was made acidic with 3 N HCl, and the precipitate was collected by filtration, washed with water and then with ethyl acetate, and dried to give **18** (0.65 g, 91%). An analytical sample was recrystallized from DMF (mp 324–326 °C): IR 3150, 1660 cm^{-1}; ^{1}H-NMR (DMSO-d_6) 4.99 (s, 2H), 7.18–7.34 (m, 3H), 7.39–7.63 (m, 3H), 8.02 (d, J = 7.5, 1H), 8.18 (d, J = 8.2, 1H), 12.02 (br s, 1H). Anal. ($C_{16}H_{11}NO_2$) C, H, N.

7-Chloro-6*H*-[1]benzopyrano[3,4-*c*]quinoline (8). A mixture of **18** (1.3 g, 5.22 mmol) in $POCl_3$ (10 mL) was refluxed for 40 min and then poured onto crushed ice. The precipitate was extracted with chloroform (3 × 50 mL), and the combined extracts were washed with water, dried over sodium sulfate, and concentrated under reduced pressure. The residue was purified by column chromatography with dichloromethane as eluent, and 93% of pure **8** (1.3 g) was obtained. Recrystallization from ethanol gave an analytical sample melting at 125–126 °C: ^{1}H-NMR ($CDCl_3$) 5.26 (s, 2H), 7.18–7.26 (m, 2H), 7.39–7.75 (m, 3H), 8.01–8.09 (m, 2H), 8.47 (d, J = 8.6, 1H). Anal. ($C_{16}H_{10}NO_2Cl$) C, H, N.

6-Chloro-7,8-dihydrobenzo[*k*]phenanthridine (10). To a solution of **21**[15] (0.5 g, 1.65 mmol) in dichloromethane (50 mL) was added aluminum chloride (1.5 g, 11.25 mmol). The reaction mixture was stirred at room temperature for 36 h and then poured into ice–water and extracted with chloroform (3 × 20 mL). The usual workup of the organic layer after evaporation under reduced pressure gave a brown oil which was purified by column chromatography using dichloromethane as eluent; **10** was obtained as a pale yellow, thick oil (0.36 g, 82%; (lit.[16a] mp 80–81 °C, lit.[16b] mp 95–96 °C): ^{1}H-NMR ($CDCl_3$) 2.85–2.92 (m, 2H), 3.01–3.10 (m, 2H), 7.37–7.42 (m, 3H), 7.52–7.59 (m, 1H), 7.66–7.73 (m, 1H), 7.89–7.93 (m, 1H), 8.07 (d, J = 8.0, 1H), 8.42 (d, J = 8.5, 1H); MS m/z 265 (M^+, 100). Anal. ($C_{17}H_{12}NCl$) C, H, N.

6-Chlorobenzo[*k*]phenanthridine (11). A mixture of **10** (1.0 g, 3.76 mmol) in carbon tetrachloride (100 mL) with *N*-chlorosuccinimide (0.51 g, 3.82 mmol) and dibenzoyl peroxide (0.1 g, 0.41 mmol) was refluxed for 5 h, filtered, and concentrated under reduced pressure. Purification of the residue by column chromatography with dichloromethane–light petroleum ether (1:1) as eluent gave **11** as a white solid (0.81 g, 82%). An analytical sample was recrystallized from ethanol–methanol (mp 106–107 °C, lit.[17a] mp 105–108 °C, lit.[16b] mp 109–110 °C, lit.[17b] mp 106–108 °C, lit.[17c] 106–107 °C): ^{1}H-NMR ($CDCl_3$) 7.69–7.83 (m, 4H), 8.03–8.11 (m, 2H), 8.20–8.25 (m, 1H), 8.41 (d, J = 8.9, 1H), 9.01 (d, J = 8.2, 1H), 9.11–9.15 (m, 1H); MS m/z 263 (M^+, 100). Anal. ($C_{17}H_{10}NCl$) C, H, N.

2-Chloro-4-phenyl-3-quinolineacetic Acid Chloride (24). A mixture of **23**[16a] (1.0 g, 3.58 mmol) in $POCl_3$ (18 mL, 0.19 mol) was refluxed for 5 h and then cooled and poured into ice–water (400 mL). The precipitate was extracted with chloroform (3 × 20 mL), and the organic layer was dried over sodium sulfate and concentrated under reduced pressure. Purification by column chromatography with dichloromethane as eluent gave **24** as a white solid (0.66 g, 58% recrystallized from hexane–cyclohexane; mp 128–129 °C): IR 1780 cm^{-1}; ^{1}H-NMR ($CDCl_3$) 4.26 (s, 2H), 7.23–7.58 (m, 7H), 7.71–7.79 (m, 1H), 8.08 (d, J = 8.4, 1H); MS m/z 315 (M^+, 33). Anal. ($C_{17}H_{11}NOCl_2$) C, H, N.

6-Chloro-8-hydroxybenzo[*k*]phenanthridine (25). To a solution of **24** (0.5 g, 1.58 mmol) in dichloromethane (150 mL) was added aluminum chloride (2.0 g, 15.0 mmol). The reaction mixture was stirred at room temperature for 6 h and then poured into ice–water. The organic solvent was removed under reduced pressure, and the precipitate was collected by filtration and dried. The yellow solid was dissolved in THF (30 mL) and filtered, and the filtrate was concentrated under reduced pressure to give **25** (0.4 g, 90%). Recrystallization from ethanol gave an analytical sample melting at 200 °C dec: ^{1}H-NMR (DMSO-d_6) 7.74 (s, 1H), 7.80–7.95 (m, 4H), 8.09–8.16 (m, 1H), 8.50–8.56 (m, 1H), 8.96–9.01 (m, 1H), 9.13–9.19 (m, 1H), 11.30 (s, 1H); MS m/z 279 (M^+, 100). Anal. ($C_{17}H_{10}NOCl$) C, H, N.

6-Chloro-8-methoxybenzo[*k*]phenanthridine (12). To a mixture of **25** (0.6 g, 2.14 mmol) in acetone (100 mL) with potassium carbonate (2.0 g, 14.47 mmol) was added methyl iodide (1.3 mL, 20.88 mmol). The mixture was refluxed for 1 h and then poured into ice–water and extracted with chloroform (3 × 20 mL). The organic layer was washed with water, dried over sodium sulfate, and evaporated under reduced pressure to give a yellow residue. Purification by column chromatography of the residue with chloroform–light petroleum ether (1:1) as eluent gave **12** (0.56 g, 89% recrystallized from ethanol–chloroform; mp 162–163 °C): ^{1}H-NMR ($CDCl_3$) 4.21 (s, 3H), 7.63 (s, 1H), 7.67–7.83 (m, 4H), 8.16–8.21 (m, 1H), 8.52–8.57 (m, 1H), 8.88–8.93 (m, 1H), 9.06–9.11 (m, 1H). Anal. ($C_{18}H_{12}NOCl$) C, H, N.

X-ray Crystallography. Single crystals of **5f,j,n** were submitted to X-ray data collection on a Siemens P4 four-circle diffractometer with graphite monochromated Mo Kα radiation. The $\omega/2\theta$ scan technique was used. The structures were solved by direct methods. The refinement was carried out by full-matrix (**5f,n**) or block-matrix (**5j**) anisotropic least-squares on F for all non-H atoms by minimizing the function $\Sigma w(|F_o| - |F_c|)^2$. The hydrogen atoms were located on Fourier difference maps and included in the structure factor calculations with an isotropic temperature factor. Atomic scattering factors including f' and f'' were taken from ref 28. Structure solution,

analysis, and refinement were carried out by using the SHELXTL PC package.[28]

5j: $C_{23}H_{23}N_3O \cdot 0.13H_2O$ (mol wt 347.6), a pale yellow, single crystal, dimensions 0.2 × 0.2 × 0.1 mm, used for data collection; monoclinic; space group $P2_1/n$ (no. 14); a = 15.009 (1), b = 16.952(2), and c = 22.124(2) Å; β = 96.02°; V = 5596.3-(9) Å^3; Z = 12; D_c = 1.24 g/cm^3; 8769 unique reflections (R_{int} = 0.026) were collected at 22 °C, of which 4369 were observed with $F > 3\sigma(F)$; no absorption correction was applied; final refinement converged to R = 0.068 and R_w = 0.075; min. and max heights in last $\Delta\rho$ map of −0.28 and 0.25 eÅ^{-3}.

5f: $C_{21}H_{21}N_3O$ (mol wt 331.4), a pale yellow, single crystal, dimensions 0.5 × 0.1 × 0.05 mm, used for data collection; monoclinic; space group $P2_1/c$ (no. 14); a = 12.415(2), b = 10.806(2), and c = 13.253(3) Å; β = 102.83°; V = 1733.6(6) Å^3; Z = 4; D_c = 1.27 g/cm^3; 3031 unique reflections (R_{int} = 0.011) were collected at 22 °C, of which 2031 were observed with $F > 3\sigma(F)$; no absorption correction was applied; final refinement converged to R = 0.052 and R_W = 0.076; min. and max heights in last $\Delta\rho$ map of −0.18 and 0.23 eÅ^{-3}.

5n: $C_{22}H_{23}N_3$ (mol wt 329.4), a yellow, single crystal, dimensions 0.2 × 0.1 × 0.05 mm, used for data collection; orthorhombic; space group $Pbcn$ (no. 60); a = 41.893(8), b = 8.290(2), and c = 10.183(2) Å; V = 3536.6(9) Å^3; Z = 8; D_c = 1.24 g/cm^3; 3106 unique reflections (R_{int} = 0.014) were collected at 22 °C, of which 1928 were observed with $F > 3\sigma(F)$; no absorption correction was applied; final refinement converged to R = 0.055 and R_W = 0.045; min. and max heights in last $\Delta\rho$ map of −0.16 and 0.16 eÅ^{-3}. Full crystallographic details will be given elsewhere.

***In Vitro* Binding Assays.** Binding assays were done as described in refs 7, 23, and 24. Male CRL:CD(SD)BR-COBS rats and male albino guinea pigs were killed by decapitation; their brains were rapidly dissected into the various areas (rat hippocampus for 5-HT$_{1A}$; rat striatum for 5-HT$_{1B}$; rat cortex for 5-HT$_{2A}$, 5-HT$_3$, and 5-HT uptake site; guinea pig striatum for 5-HT$_4$) and stored at −80 °C until the day of assay. The pig brain was obtained from a local slaughterhouse; cortex (for 5-HT$_{2C}$) was rapidly removed and stored at −80 °C until the day of assay. Tissues were homogenized in 50 vol of ice-cold Tris HCl, 50 mM, pH 7.4 (or Hepes HCl, 50 mM, pH 7.4, for 5-HT$_4$ and 5-HT$_3$ receptors), using an Ultra Turrax TP-1810 homogenizer (2 × 20 s), and homogenates were centrifuged at 50000g for 10 min (Beckman model J-21B refrigerated centrifuge). Each pellet was resuspended in the same volume of fresh buffer, incubated at 37 °C for 10 min, and centrifuged again at 50000g for 10 min. The pellet was then washed once by resuspension in fresh buffer and centrifuged as before. The pellet obtained was finally resuspended in the appropriate incubation buffer (Tris HCl, 50 mM, pH 7.7, containing 10 μM pargyline and 4 mM $CaCl_2$ for 5-HT$_{1A}$ receptors; Tris HCl, 50 mM, pH 7.7, containing 10 μM pargyline, 4 mM $CaCl_2$, and 0.1% ascorbic acid for 5-HT$_{1B}$ and 5-HT$_{2C}$ receptors; Tris HCl, 50 mM, pH 7.7, for 5-HT$_{2A}$ receptors; Tris HCl, 50 mM, pH 7.4, containing 10 μM pargyline, 120 mM NaCl, and 5 mM KCl for 5-HT uptake site; Hepes HCl, 50 mM, pH 7.4, containing 10 μM pargyline for 5-HT$_3$ and 5-HT$_4$ receptors) just before the binding assay.

[^{3}H]-8-OH-DPAT (SA 157.4 Ci/mmol, for 5-HT$_{1A}$; NEN) and [^{3}H]citalopram (SA 73.7 Ci/mmol, for 5-HT uptake site; NEN) binding was assayed in a final incubation volume of 0.5 mL, consisting of 0.25 mL of membrane suspension, 0.24 mL of the [^{3}H]ligand, and 0.01 mL of displacing agent or solvent. Tissue concentration and [^{3}H]ligand final concentration were respectively 5 mg of tissue/sample and 1 nM, and 3.1 mg of tissue/sample and 0.8 nM. [^{3}H]Mesulergine (SA 73.0 Ci/mmol, for 5-HT$_{2C}$; NEN), [^{3}H]-5-HT (SA 14.6 Ci/mmol,for 5-HT$_{1B}$; NEN), [^{3}H]ketanserin (SA 60.0 Ci/mmol, for 5-HT$_{2A}$; Amersham), [^{3}H]-BRL43694 (SA 84.8 Ci/mmol, for 5-HT$_3$; NEN), and [^{3}H]GR 113808[24] (SA 84.0 Ci/mmol, for 5-HT$_4$; Amersham) binding was assayed in a final incubation volume of 1.0 mL, consisting of 0.5 mL of membrane suspension, 0.48 mL of the [^{3}H]ligand, and 0.02 mL of displacing agent or solvent. Tissue concentration and [^{3}H]ligand final concentration were 33 mg/sample and 1 nM ([^{3}H]mesulergine binding), 10 mg/sample and 2 nM ([^{3}H]-5-HT binding), 5 mg/sample and 0.7 nM ([^{3}H]ketanserin binding), 20 mg/sample and 1 nM ([^{3}H]BRL43694 binding), and 30 mg/sample and 0.1 nM ([^{3}H]GR 113808 binding).

Incubations were stopped by rapid filtration under vacuum through GF/B or GF/C filters which were then washed with 12 mL (4 × 3 times) of ice-cold Tris HCl, 50 mM, pH 7.4, or Hepes HCl, 50 mM, pH 7.4, using a Brandel M-48R cell harvester. Dried filters were immersed in vials containing 4 mL of Filter Count (Packard) for the measurement of trapped radioactivity with an LKB1214 RACKBETA liquid scintillation spectrometer at a counting efficiency of about 60%. Dose–inhibition curves were analyzed by the "Allfit" program[29] to obtain the concentration of unlabeled drug that caused 50% inhibition of ligand binding. The K_i values were derived from the IC_{50} values according to the method of Cheng and Prusoff.[30] The K_d (nM) values of the radiolabeled ligands used were obtained from the literature[23,24,31] and were 0.9 for [^{3}H]-8-OH-DPAT binding, 1.9 for [^{3}H]-5-HT binding, 3.2 for [^{3}H]mesulergine binding, 0.5 for [^{3}H]ketanserin binding, 2.0 for [^{3}H]citalopram binding 0.3 for [^{3}H]BRL43694 binding, and 0.2 for [^{3}H]GR 113808 binding.

Measurement of [^{14}C]Guanidinium Uptake in NG 108-15 Cells. This procedure has been described by Emerit et al.[8] as a convenient assay for assessing the agonist/antagonist activity of drugs acting at 5-HT$_3$ receptors. Thus, 5-HT$_3$ receptor agonists markedly enhance [^{14}C]guanidinium uptake by these cells, and this response is selectively blocked by 5-HT$_3$ receptor antagonists.[8] Briefly, mouse neuroblastoma x rat glioma hybrid cells of the NG 108-15 clone were grown in Dulbecco's modified Eagle's medium supplemented with the appropriate nutrients[8] for 2 days. The cell layer in each culture dish (35 mm) was then washed twice with 1.5 mL of buffer A (145 mM NaCl, 5.4 mM KCl, 1.8 mM $CaCl_2$, 1.0 mM $MgCl_2$, 2.0 mM Na_2HPO_4, 20 mM glucose, 20 mM HEPES, pH adjusted to 7.4 with NaOH) and covered with 1 mL of buffer B (same composition as buffer A except that [NaCl] was reduced to 135 mM and 10 mM guanidinium was added) containing 0.20–0.25 μCi of [^{14}C]guanidinium (SA 59 mCi/mmol; Service des Molécules Marquées at CEA, 91191 Gif-surYvette, France) and, where indicated, 1 μM 5-HT, 10 μM substance P, and/or eight different concentrations of each drug to be tested. After 10 min at 37 °C, the assay was stopped by aspiration of the medium, and the cell layer was washed three times with 1.5 mL of ice-cold buffer C (same composition as buffer A except that NaCl was replaced by choline chloride). The cells were then dissolved in 0.5 mL of 0.4 M NaOH, and the resulting extracts were transferred to scintillation vials. The culture dishes were further rinsed with 0.5 mL of 1 M HCl and then with 0.5 mL of 0.4 M NaOH, which was added to the vials. Each mixture (1.5 mL) was supplemented with 10 mL of the scintillation fluid Aquasol (New England Nuclear, Les Ulis, France) for radioactivity counting at 50% efficiency. All assays were performed in triplicate.

Under these conditions, [^{14}C]guanidinium accumulation in NG 108-15 cells was 4–5 times higher in the presence of both 1 μM 5-HT and 10 μM substance P than in their absence (basal uptake). 5-HT$_3$ receptor antagonists (zacopride, ondansetron, tropisetron, etc) completely prevented the stimulatory effect of 5-HT (with substance P) (see ref 8 for details).

Bezold–Jarisch Reflex. The stimulation of cardiac 5-HT$_3$ receptors is well known to trigger a transient bradycardia known as the Bezold–Jarisch reflex[9] in urethane-anesthetized rats. The ability of drugs to either induce or prevent this reflex has been used to further assess the 5-HT$_3$ receptor agonist or antagonist properties of the newly synthesized arylpiperazine derivatives. Briefly, adult male Sprague–Dawley rats (250–300 g body weight; Centre d'Elevage R. Janvier, Le Genest, France) were anesthetized with urethane (1.4 g/kg ip), and a tracheotomy was performed to insert an endotracheal tube. A catheter (0.3 mm internal diameter) was inserted into the abdominal aorta via the femoral artery in order to record the arterial pressure and heart rate. A femoral vein was exposed and cannulated for iv injection of drugs. The Bezold–Jarisch reflex (which consists of a 60% drop in heart rate within 10–15 s following the injection of 30 μg/kg iv serotonin) was assessed 5, 15, and 30 min after the iv administration of various doses of each arylpiperazine derivative. Under these

conditions, 10 μg/kg iv of either zacopride, ondansetron, or tropisetron injected 5 min before 5-HT completely prevented the bradycardia normally evoked by the indoleamine.[9]

Acknowledgment. Thanks are due to Italian MURST and French INSERM and DRET (Contract No. 93.047) for financial support.

References

(1) Kilpatrick, G. J.; Bunce, K. T.; Tyers, M. B. 5-HT_3 Receptors. *Med. Res. Rev.* **1990**, *10*, 441–475 and references cited therein.
(2) Van Wijngaarden, I.; Hamminga, D.; Van Hes, R.; Standaar, P. J.; Tipker, J.; Tulp, M. Th. M.; Mol, F.; Olivier, B.; De Jonge, A. Development of High-Affinity 5-HT_3 Receptor Antagonists. Structure Affinity Relationships of Novel 1,7-Annelated Indole Derivatives.1. *J. Med. Chem.* **1993**, *36*, 3693–3699 and references cited therein.
(3) (a) Milburn, C. M.; Peroutka, S. Characterization of [^{3}H]-Quipazine Binding to 5-Hydroxytryptamine$_3$ Receptors in Rat Brain Membranes. *J. Neurochem.* **1989**, *52*, 1787–1792. (b) Fozard, J. R. 5-HT_3 Receptors in the context of the multiplicity of 5-HT Receptors. In *Central and Peripheral 5-HT_3 Receptors*; Hamon, M., Ed.; Academic Press:, London, 1992; pp 1–12.
(4) Costall, B.; Naylor, J. R.; Tyers, B. M. The Psychopharmacology of 5-HT_3 Receptors. *Pharmacol. Ther.* **1990**, *47*, 181–202.
(5) Anzini, M.; Vomero, S.; Garofalo, A.; Cappelli, A.; Cagnotto, A. Synthesis and 5-HT Receptor Affinity of Some 4-Phenylquinoline Derivatives. *Farmaco* **1989**, *44*, 555–563.
(6) (a) Anzini, M.; Cappelli, A.; Vomero, S.; Campiani, G.; Cagnotto, A.; Skorupska, M. Synthesis and 5-HT Receptor Binding Studies of Some 3-Substituted-2-(4-methyl-1-piperazinyl)-4-phenylquinolines. *Farmaco* **1991**, *46*, 1435–1447. (b) Anzini, M.; Cappelli, A.; Vomero, S. Synthesis of 6-(4-Methyl-1-piperazinyl)-7H-indeno[2,1-c]quinoline Derivatives as Potential 5-HT Receptor Ligands. *J. Heterocycl. Chem.* **1991**, *28*, 1809–1812. (c) Anzini, M.; Cappelli, A.; Vomero, S. Synthesis of 6,7-Dihydro-8-(4-methyl-1-piperazinyl)[1]benzoxepino[4,5-c]quinoline as Potential 5-HT_3 Receptor Ligands. *Heterocycles* **1993**, *36*, 1065–1074.
(7) Anzini, M.; Cappelli, A.; Vomero, S.; Cagnotto, A.; Skorupska, M. 6-(1-Piperazinyl)-7H-indeno[2,1-c]quinoline Derivatives with High Affinity and Selectivity for 5-HT_3 Serotonin Sites. *Med. Chem. Res.* **1993**, *3*, 44–51.
(8) Emerit, M. B.; Riad, M.; Fattaccini, C. M.; Hamon, M. Characteristics of [^{14}C]Guanidinium Accumulation in NG 108–15 Cells Exposed to Serotonin 5-HT_3 Receptor Ligands and Substance P. *J. Neurochem.* **1993**, *60*, 2059–2067.
(9) Cohen, M. L.; Bloomquist, W.; Gidda, J. S.; Lacefield, W. Comparison of the 5-HT_3 Receptor Antagonist Properties of ICS 205–930, GR38032F and Zacopride. *J. Pharmacol. Exp. Ther.* **1989**, *248*, 197–201.
(10) Blackburn, T. P.; Cox, B.; Guildford, A. J.; Le Count, D. J.; Middlemiss, D. M.; Pearce, R. J.; Thornbee, C. W. Synthesis and 5-Hydroxytryptamine Antagonist Activity of 2-[[2-(Dimethylamino)ethyl]thio]-3-phenylquinoline and Its Analogues. *J. Med. Chem.* **1987**, *30*, 2252–2259.
(11) Yamaguchi, S.; Oh-Hino, Y.; Yamada, M.; Michitani, H.; Kawase, Y. The synthesis of Benzofuroquinolines. VI. A New Synthesis of Benzofuro[2,3-c]quinoline Derivatives. *Bull. Chem. Soc. Jpn.* **1990**, *63*, 952–954.
(12) Walser, A.; Silverman, G.; Flynn, T.; Fryer, R. I. Nucleophilic Displacement of Aromatic Fluorine, Part III, Indoloquinolines and Benzofuranoquinolines. *J. Heterocycl. Chem.* **1975**, *12*, 351–352.
(13) In order to avoid the tedious purification of rather insoluble compound **15** by chromatography, the crude mixture obtained from the cyclization of chloroacetamide **14** was recrystallized from ethanol and used without further handling in the next cyclization step. The presence of compound **16** did not seem to affect the cyclization reaction course. Furthermore rather insoluble compound **17** could be easily purified from unreacted **16** and some other impurities simply by washing with hot ethyl acetate.
(14) Walser, A.; Flynn, T.; Fryer, R. I. Nucleophilic Displacement of Aromatic Fluorine, Part IV, Quinolinoquinolines and Benzochromanoquinolines. *J. Heterocycl. Chem.* **1975**, *12*, 737–741.
(15) Ramasamy, K.; Shanmugam, P. Tellurium Heterocycles, I. Synthesis of 2,3-Dihydrotellurolo[2,3-b]quinolines. *Naturforschung* **1977**, *32b*, 605–606.
(16) (a) Paramasivam, K.; Ramasamy, K.; Shanmugam, P. Furoquinolines; Part XI, A Novel $AlCl_3$-Catalysed Rearrangement of 4-Phenyl-2,3-dihydrofuro[2,3-b]quinolines. A New Route to the 5,6-Benzophenanthridine System. *Synthesis* **1977**, 768–770. (b) Veeramani, K.; Paramasivam, K.; Ramakrishnasubramanian, S.; Shanmugam, P. Photolysis of 4-Phenyl-3-vinylquinolines; A Facile New Route to the Benzo[k]phenanthridine System. *Synthesis* **1978**, 855–857.
(17) (a) Keene, B. R. T.; Schofield, K. The Ring Expansion of 3:4-Benzofluorenone by Hydrazoic Acid. *J. Chem. Soc.* **1958**, 2609–2612. (b) Arisvaran, V.; Ramesh, M.; Rajendran, S. P.; Shanmugan, P. Synthesis of Benzo[k]phenanthridines: Another New Approach. *Synthesis* **1981**, 821–823. (c) Veeramani, K.; Shanmugam, P. *Indian J. Chem.* **1987**, *26B*, 116–121.
(18) Sybyl 6.03, Tripos Assoc., 1699 S. Hanley Rd., Suite 303, St. Louis, MO 63144.
(19) Clark, M.; Cramer, R. D., III; Van Opdenbosch, N. Validation of the General Purpose TRIPOS 5.2 Force Field. *J Comput. Chem.* **1989**, *10*, 982–1012.
(20) Gasteiger, J.; Marsili, M. Iterative Partial Equalization of Orbital Electronegativity - A Rapid Access to Atomic Charges. *Tetrahedron* **1980**, *36*, 3219–3228.
(21) Cramer, R. D., III; Patterson, D. E.; Bunce, J. D. Comparative Molecular Field Analysis (CoMFA). Effect of Shape of Binding of Steroid to Carrier Proteins. *J. Am. Chem. Soc.* **1988**, *110*, 5959–5967.
(22) Wold, S.; Ruhe, A.; Wold, H.; Dunn, W. J. The Covariance Problem in Linear Regression. The Partial Least-Squares (PLS) Approach to Generalized Inverses. *SIAM J. Sci. Stat. Comput.* **1984**, *5*, 735–743.
(23) (a) Mennini, T.; Bizzi, A.; Caccia, S.; Codegoni, A.; Fracasso, C.; Frittoli, E.; Guiso, G.; Padura, I. M.; Taddei, C.; Uslenghi, A.; Garattini, S. Comparative Studies on the Anoretic Activity of d-Fenfluramine in Mice, Rats and Guinea Pigs. *Arch. Pharmacol.* **1991**, *343*, 483–490. (b) Caccia, S.; Anelli, M.; Fracasso, C.; Frittoli, E.; Giorcelli, P.; Gobbi, M.; Taddei, C.; Garattini, S.; Mennini, T. Anorectic Effect and Brain Concentrations of d-Fenfluramine in the Marmoset: Relationship to the In Vivo and In Vitro Effects on Serotonergic Mechanism. *Arch. Pharmacol.* **1993**, *347*, 306–312.
(24) Grossman, C. J.; Kilpatrick, G. J.; Bunce, K. T. Development of a Radioligand Binding Assay for 5-HT_4 Receptors in Guinea Pig and Rat Brain. *Br. J. Pharmacol.* **1993**, *109*, 618–624.
(25) The K_i values of compounds **4a,b** and **26** were calculated from the reported IC_{50} values (see ref 7) according to the method of Cheng and Prusoff (see ref 30).
(26) The default parameters of the Sybyl[18] molecular dynamics option were used; conformers were collected every 100 fs for a period of 200 ps at 300 K.
(27) Bockaert, J.; Ansanay, H.; Waeber, C.; Sebben, M.; Fagni, L.; Dumuis, A. 5-HT_4 Receptors. Potential Therapeutic Implications in Neurology and Psychiatry. *CNS Drugs* **1994**, *1*, 6–15.
(28) SHELXTL PC, Siemens Analytical X-Ray Instruments, Inc., Madison, WI; Rel. 4.1, 1990.
(29) De Lean, K. W.; Munson, P. J.; Rodbard, D. Simultaneous Analysis of Families of Sigmoidal Curves: Application to Bioassay, Radioligand Assay and Physiological Dose-Response Curves. *Am. J. Physiol.* **1978**, *235*, E97–E102.
(30) Cheng, Y.; Prusoff, W. H. Relationship between the Inhibition Constant (Ki) and the Concentration of Inhibitor Which Causes 50 Per Cent Inhibition (IC_{50}) of an Enzymatic Reaction. *Biochem. Pharmacol.* **1973**, *22*, 3099–3108.
(31) Nelson, D. R.; Thomas, D. R. [^{3}H]-BRL 43694 (Granisetron) a Specific Ligand for 5-HT_3 Binding Sites in Rat Brain Cortical Membranes. *Biochem. Pharmacol.* **1989**, *38*, 1693–1695.

JM950019Q